Fussing about fission: defining variety among mainstream and exotic apicomplexan cell division modes

Marc-Jan Gubbels[1§], Caroline D. Keroack[2], Sriveny Dangoudoubiyam[3*], Hanna L. Worliczek[1,4,#], Aditya S. Paul[2], Ciara Bauwens[1], Brendan Elsworth[2,5], Klemens Engelberg[1], Daniel K. Howe[3], Isabelle Coppens[6], Manoj T. Duraisingh[2§]

[1] Department of Biology, Boston College, Chestnut Hill, MA

[2] Department of Immunology and Infectious Diseases, Harvard T. H. Chan School of Public Health, Harvard University, Boston, MA

[3] Gluck Equine Research Center, Department of Veterinary Science, University of Kentucky, Lexington, KY

[4] Institute of Parasitology, University of Veterinary Medicine, Vienna, Austria

[5] School of Biosciences, University of Melbourne, Melbourne, Australia

[6] Department of Molecular Microbiology and Immunology, Bloomberg School of Public Health, Johns Hopkins University, Baltimore, MD

[§] **Correspondence:**
Marc-Jan Gubbels
gubbelsj@bc.edu

Manoj T. Duraisingh
mduraisi@hsph.harvard.edu

*present address: Department of Comparative Pathobiology, Purdue University College of Veterinary Medicine, West Lafayette, IN

[#]present address: Department of History, University of Vienna, Vienna, Austria

Keywords: Apicomplexa, cell division, cell cycle, karyokinesis, schizogony, endodyogeny, endopolygeny, binary fission

Abstract

Cellular reproduction defines life, yet our textbook-level understanding of cell division is limited to a small number of model organisms centered around humans. The horizon on cell division variants is expanded here by advancing insights on the fascinating cell division modes found in the Apicomplexa, a key group of protozoan parasites. The Apicomplexa display remarkable variation in offspring number, whether karyokinesis follows each S/M-phase or not, and whether daughter cells bud in the cytoplasm or bud from the cortex. We find that the terminology used to describe the various manifestations of asexual apicomplexan cell division emphasizes either the number of offspring or site of budding, which are not directly comparable features and has led to confusion in the literature. Division modes have been primarily studied in two human pathogenic Apicomplexa, malaria-causing *Plasmodium* spp. and *Toxoplasma gondii*, a major cause of opportunistic infections. *Plasmodium* spp. divide asexually by schizogony, producing multiple daughters per division round through a cortical budding process, though at several life-cycle nuclear amplifications are not followed by karyokinesis. *T. gondii* divides by endodyogeny producing two internally budding daughters per division round. Here we add to this diversity in replication mechanisms by considering the cattle parasite *Babesia bigemina* and the pig parasite *Cystoisospora suis*. *B. bigemina* produces two daughters per division round by a 'binary fission' mechanism whereas *C. suis* produces daughters through both endodyogeny and multiple internal budding known as endopolygeny. In addition, we provide new data from the causative agent of equine protozoal myeloencephalitis (EPM), *Sarcocystis neurona*, which also undergoes endopolygeny but differs from *C. suis* by maintaining a single multiploid nucleus. Overall, we operationally define two principally different division modes: internal budding found in cyst-forming Coccidia (comprising endodyogeny and two forms of endopolygeny) and external budding found in the other parasites studied (comprising the two forms of schizogony, binary fission and multiple fission). Progressive insights into the principles defining the molecular and cellular requirements for internal versus external budding, as well as variations encountered in sexual stages are discussed. The evolutionary pressures and mechanisms underlying apicomplexan cell division diversification carries relevance across Eukaryota.

60

61 **Contribution to the Field**

62

63 Mechanisms of cell division vary dramatically across the Tree of Life, but the mechanistic basis
64 has only been mapped for several model organisms. Here we present cell division strategies
65 across Apicomplexa, a group of obligate intracellular parasites with significant impact on
66 humans and domesticated animals. Asexual apicomplexan cell division is organized around
67 assembly of daughter buds, but division forms differ in the cellular site of budding, number of
68 offspring per division round, whether each S-phase follows karyokinesis and if mitotic rounds
69 progress synchronously. This varies not just between parasites, but also between different life-
70 cycle stages of a given species. We discuss the historical context of terminology describing
71 division modes, which has led to confusion on how different modes relate to each other.
72 Innovations in cell culture and genetics together with light microscopy advances have opened up
73 cell biological studies that can shed light on this puzzle. We present new data for three division
74 modes barely studied before. Together with existing data, we show how division modes are
75 organized along phylogenetic lines and differentiate along external and internal budding
76 mechanisms. We also discuss new insights into how the variations in division mode are regulated
77 at the molecular level, and possess unique cell biological requirements.

78 **1 Introduction**

79 Reproduction is critical for perpetuating a species and lies at the core of the definition of life.
80 Yet, the modes by which cell division can occur are very diverse. The molecular and cellular
81 mechanisms underlying such differences have been dissected for a limited set of model
82 organisms, most of which carry resemblance to mammalian/human cell division. The
83 Apicomplexa comprise a protozoan phylum harboring human pathogens, like malaria-causing
84 *Plasmodium* spp., opportunistic parasites like *Toxoplasma gondii* and *Cryptosporidium* spp., and
85 emerging pathogens like *Babesia* spp. (phylogeny in Fig 1). In addition, many are of economic
86 relevance in agriculture and companion animals such as *Babesia* spp, *Theileria* spp. and *Eimeria*
87 spp. Furthermore, many Apicomplexa infect other birds, mammals, reptiles, amphibians, fish,
88 and invertebrates, but their cell biology has only been studied minimally. The asexual
89 multiplication cycles of the Apicomplexans are diverse, and their sexual cycles add even more
90 diversity. The well-studied Apicomplexa relevant to humans display a diverse spectrum of
91 asexual cell division strategies both within and among species, providing an excellent
92 opportunity for comparative biology. Indeed, we posit that by studying the principles in more
93 distant organisms such as protozoa, which span a wide breadth of evolutionary history and
94 correspondingly diverse biology, we can obtain fascinating new insights and principles.

95 Asexual apicomplexan cell division revolves around variations in budding through the
96 assembly of a membrane skeleton that ultimately underlies the plasma membrane. The
97 beginning- and end-point of a cell division round across all Apicomplexa is a "zoite", a cell type
98 with the phylum-defining complex of apical secretory organelles and cytoskeletal structures
99 (Leander and Keeling, 2003) (e.g. Fig 2A, 3F1, 4A, 5E1, 6C1). These apical structures uniformly
100 facilitate host-cell invasion, an essential step in the obligate intracellular life style of
101 apicomplexan parasites (Gubbels and Duraisingh, 2012; Sharma and Chitnis, 2013; Frenal et al.,
102 2017a). The cortical cytoskeleton just below the plasma membrane, however, plays an additional
103 role as a key structure facilitating budding across asexual division modes for Apicomplexa
104 (Anderson-White et al., 2012; Kono et al., 2016). From the outside in, it is built up from three
105 uniformly conserved elements: alveolar vesicles (alveoli) that anchor the myosin motor enabling
106 motility (Frenal et al., 2017a), an epiplastin (a.k.a. alveolar) protein meshwork (Goodenough et
107 al., 2018), and a series of sub-pellicular, longitudinal microtubules emanating from the apical
108 end. The number and length of the microtubules vary across parasite species and stage (Spreng et

109 al., 2019), but the alveoli and epiplastin meshwork are universally conserved and make up the
110 inner membrane complex (IMC) (Kono et al., 2012). The epiplastin family proteins contain Val-
111 Pro-Val (VPV) repeats and are generally known as alveolins or IMC proteins (Gould et al., 2008;
112 Anderson-White et al., 2011; Kono et al., 2012; Al-Khattaf et al., 2015). Cytoskeletal assembly
113 initiates from the centrosome and all three elements are simultaneously assembled in an apical to
114 basal direction (Chen and Gubbels, 2013; Francia and Striepen, 2014; Suvorova et al., 2015).
115 Another important and shared feature is that across asexual division modes, budding appears to
116 be tied always to a round of S-phase and mitosis (Francia and Striepen, 2014; Suvorova et al.,
117 2015). A fourth cytoskeleton element that is conserved across division modes is the basal
118 complex, a ring residing at the basal end of the daughter bud (Ferguson et al., 2008). This ring
119 contains MORN1, a scaffolding protein that is essential for maintenance of the daughter bud's
120 basal end integrity (Gubbels et al., 2006; Hu, 2008; Heaslip et al., 2010; Lorestani et al., 2010;
121 Kono et al., 2016). Proteins with repetitive MORN domains are often found in cilia and flagella
122 (Mecklenburg, 2007; Shetty et al., 2007; Tokuhiro et al., 2008; Morriswood and Schmidt, 2015);
123 indeed all apicomplexan division modes share several features with cilia or flagella assembly as
124 seen across eukaryotes. For example, striated fiber assembly (SFA) fibers are found in flagellar
125 assembly in algae to orient the basal body in the flagellum, which in Apicomplexa anchor the
126 centrosome in the daughter bud (Francia et al., 2012). A spindle assembly abnormal protein 6
127 (SAS6)-like protein found in flagellar basal bodies is also found in the apical polar ring (APR),
128 the microtubule organizing center (MTOC) nucleating the subpellicular microtubules (and
129 conoid, if present) (de Leon et al., 2013; Francia et al., 2015; Wall et al., 2016). Finally, the base
130 of cilia and flagella is often decorated with a contractile centrin and a myosin (Roberts et al.,
131 2004; Trojan et al., 2008), which, at least in *T. gondii*, are represented by TgCentrin2 and
132 Myosin I and J (Hu et al., 2006; Hu, 2008; Frenal et al., 2017b).
133 Despite this central plan, many variations exist on what precedes daughter budding, and how
134 daughter bud formation is orchestrated. The first variable is the number of offspring per mother
135 cell in an asexual apicomplexan division round, which can be as few as two or nearly 100,000.
136 The principle behind the uncoupling of daughter formation from S/M-phase was recently
137 established in *T. gondii* by the presence of a bipartite centrosome: the centrosome's inner-core
138 proximal to the nucleus regulates the S/M cycle independently of the centrosome's outer-core
139 distal from the nucleus, which organizes daughter bud formation (Chen and Gubbels, 2013;

140 Suvorova et al., 2015; Chen and Gubbels, 2019). Moreover, cyclins and cyclin-dependent
141 kinases (CDKs), as found in higher eukaryotes, ultimately control cell cycle progression but their
142 nature and modes of operation are specifically tailored to the needs of different apicomplexan
143 cell cycle variation (e.g. (Roques et al., 2015; Alvarez and Suvorova, 2017; Ganter et al., 2017;
144 Naumov et al., 2017), recently reviewed in (Matthews et al., 2018; White and Suvorova, 2018)).
145 A second variable is whether karyokinesis follows each S-phase and mitosis (S/M-phase) or not.
146 Finally, daughters can either assemble within the mother's cytoplasm (internal budding), or
147 assemble and emerge directly from the plasma membrane of the mother cell (cortical or
148 peripheral budding). Strikingly, these modes can vary not only between Apicomplexa, but also
149 across different life-cycle stages within a single species.
150 Although these insights describe the key principles, the details on cell biological mechanisms
151 facilitating the various division modes are intermittent and often compounded by historical
152 terminology which either do not accurately capture the shared principles or clearly define
153 differences. Here we highlight the best-understood cell division modes, schizogony in
154 *Plasmodium* spp. and endodyogeny in *T. gondii*, supplemented with new data on emerging
155 systems displaying different forms of endopolygeny in *Cystoisopora suis* and *Sarcocystis*
156 *neurona*, as well as binary fission in *Babesia bigemina*. Emerging insights are subsequently used
157 to assess their kinship and to chart principles underlying these distinct cell division modes.
158

159 **2 Material and Methods**

160 **2.1 *Babesia* spp. culture**

161 *B. bigemina* strain JG-29 (Mexico) was kindly provided by Dr. David Allred (University of
162 Florida) and grown as described previously (Vega et al., 1985) with modifications as described
163 here. Parasites were culture adapted over a month to grow efficiently in tissue culture media
164 RPMI-1640 supplemented with 25 mM HEPES, 50 mg/l hypoxanthine, 2.42 mM sodium
165 bicarbonate, and 4.31 mg/ml AlbuMAX-II (Invitrogen). Before addition of AlbuMAX-II and
166 sodium bicarbonate, the pH was adjusted to 6.75. Parasites were grown under microaerophilous
167 stationary phase culture conditions with a hypoxic atmosphere of 1:5:94 oxygen: carbon dioxide:
168 nitrogen at 4% hematocrit in washed, defibrinated bovine red blood cells (Hemostat Labs, Dixon,
169 CA).

170 *B. divergens* strain Rouen 1987, a kind gift from Drs. Kirk Deitsch and Laura Kirkman
171 (Weill Cornell Medical College), was grown in human erythrocytes as described (Paul et al.,
172 2016). Human erythrocytes were purchased from Research Blood Components (Boston, USA).
173

174 **2.2 *Cystoisospora suis* culture**

175 Oocysts of *C. suis* strain Wien-I (Austria) were isolated from porcine fecal samples and used for
176 *in vitro* culture in intestinal porcine epithelial cells (IPEC-J2, ACC 701, Leibniz Institute DSMZ
177 GmbH, Braunschweig, Germany) as described previously (Worliczek et al., 2013) with
178 modifications as described here. For the production of glass cover slips with confluent layers of
179 host cells infected with *C. suis*, cover slips were placed into 6-well culture plates for suspension
180 cultures (PAA, Pasching, Austria). IPEC-J2 were suspended in DMEM/Ham's F12 medium
181 (PAA, Austria) supplemented with 5 % fetal calf serum, 2 mM L-glutamine, 100 U/ml penicillin
182 and 0.1 mg/ml streptomycin, and seeded in a density of $4x10^5$ cells/well. After overnight
183 incubation at 37°C, 5 % CO_2 cover slips with attached IPEC-J2 were transferred to 6-well
184 surface-treated culture plates for adherent cells (PAA, Austria). Sporozoites of *C. suis* were
185 excysted as described previously (Worliczek et al., 2013), suspended in culture medium and
186 applied to the host cells in a density of sporozoites:host cells of 1:30. The infected cell cultures
187 were incubated at 37°C, 5% CO_2 and culture medium was exchanged at 1, 4, and 7 days post
188 infection (dpi).
189

190 **2.3 *S. neurona* culture and immunofluorescence assays**

191 *S. neurona* strain SN3 was cultured, transfected and processed for immunofluorescence as
192 described before (Dubey et al., 2017; Howe et al., 2018). In short, parasites were cultured and
193 maintained in bovine turbinate (BT) cell monolayers. For IFA, extracellular merozoites were
194 used to infect BT cells in 24-well plates containing coverslips. Typically, on day 3 post infection,
195 infected BT cell monolayers were methanol-fixed for downstream immunofluorescence
196 experiments. Freshly isolated extracellular *S. neurona* merozoites were used for transient
197 expression of YFP-tagged TgIMC15 (Anderson-White et al., 2011).
198

199 **2.4 *B. bigemina* immunofluorescence assays**

200 *B. bigemina* indirect immunofluorescence assays were performed on >10% parasitemia bovine
201 red blood cells by air drying drops in 10-well slides (Electron Microscopy Sciences), followed
202 by 100% methanol fixation for 5 min at -20ºC, 3 rinses in PBS and blocking in 3% BSA in PBS
203 for 1 hr at RT. Primary antibodies diluted in blocking solution (rabbit TgCentrin1 1:4000 (Fung
204 et al., 2012), mouse MAb 12G10 α-tubulin 1:100 (University of Iowa Hybridoma Bank) (Jerka-
205 Dziadosz et al., 1995); mouse ascites MAb B-5-1-2 α-tubulin 1:200 (Sigma-Aldrich #T5168); rat
206 TgEB1 1:100 (Chen and Gubbels, 2019); guinea pig BbIMC1a 1:500) were incubated for 1 hr at
207 RT, followed by 3 washes for 5 min in PBS, Alexa488 or 594 conjugated secondary antisera
208 (ThermoFisher) diluted 1:400 in 0.1% BSA in PBS for 45 min at RT followed by 1 wash for 5
209 min in PBS containing 1.5 µg/ml 4',6-diamidino-2-phenylindole (DAPI) to stain DNA, and two
210 additional 5 min washes with PBS before mounting with Fluoro-Gel (Electron Microscopy
211 Sciences). A Zeiss Axiovert 200 M wide-field fluorescence microscope was used to collect
212 images, which were deconvolved and adjusted for phase contrast using Volocity software
213 (Quorum Technologies). SR-SIM was performed on a Zeiss ELYRA S.1 system in the Boston
214 College Imaging Core in consultation with Bret Judson. All images were acquired, analyzed and
215 adjusted using ZEN software and standard settings.
216

217 **2.5 *C. suis* indirect immunofluorescence assays**

218 *C. suis* indirect immunofluorescence assays were performed on infected IPEC-J2 cells grown on
219 glass cover slips as described above at dpi 7 and 8. Infected cells on cover slips were washed in
220 PBS, fixed with ice cold methanol for 10 min and subsequently washed twice with PBS.
221 Blocking was performed for 20 min with Superblock® T20 (PBS) blocking buffer (Thermo
222 Scientific) with 1% (v/v) normal goat serum at RT. Primary antibodies (guinea pig TgNuf2
223 (Farrell and Gubbels, 2014); mouse mAb 6-11B-1 acetylated α-tubulin, Invitrogen) were diluted
224 to 1:1000 (v/v) in blocking solution, and incubated for 90 min at 37°C, followed by 2x10 min
225 washes with PBS-Tween 20 (0.01%, v/v), incubation with secondary antibodies diluted 1:600 in
226 blocking solution for 40 min at 37°C, 2x10 min washes with PBS-Tween 20, followed by 1 wash
227 for 5 min in PBS containing 1 µM DAPI, 4 washes of 5 min at RT with PBS and quick
228 immersion in ddH_2O, before mounting with Aqua Polymount (Fisher Scientific). Mounted
229 samples were hardened for 2-5 days before imaging. A Zeiss LSM 510 Meta with a 63x plan
230 apochromat oil immersion objective was used to collect Z-stacks using ZEN 2009 Light Edition

231 (Carl Zeiss Microimaging GmbH, Jena, Germany). Z-stacks were subsequently deconvoluted
232 using Huygens Essential 4.3 software (Scientific Volume Imaging Inc., The Netherlands) with
233 measured point spread functions (PSF) for the respective channels. Z-projections (maximum
234 intensity projections of split channels) were computed with ImageJ 1.48e (National Institutes of
235 Health, Bethesda, MD, USA).
236

237 **2.6 Transmission electron microscopy**

238 For thin-section transmission, pellets of >10% parasitemia *B. bigemina* infected bovine red blood
239 cells were fixed with 2.5% glutaraldehyde in 0.1 M sodium cacodylate (Sigma) buffer (pH 7.4)
240 for 1 hr at RT and processed as described (Nishikawa et al., 2005) before examination with a
241 Philips CM120 Electron Microscope (Eindhoven, The Netherlands) under 80 kV.
242 Pellets of >10% parasitemia *B. divergens* infected human red blood cells were fixed with 2.5%
243 glutaraldehyde 1.25% paraformaldehyde and 0.03% picric acid in 0.1 M sodium cacodylate buffer
244 (pH 7.4) overnight at 4°C. Cells were washed in 0.1 M cacodylate buffer and post fixed with 1%
245 OsO_4/1.5% $KFeCN_6$ for 1 hr, washed 2x in water, 1x maleate buffer (MB) 1x and incubated in 1%
246 uranyl acetate in MB for 1 hr followed by 2 washes in water and subsequent dehydration in grades
247 of alcohol (10 min each; 50%, 70%, 90%, 2x10 min 100%). The samples were then put in
248 propyleneoxide for 1 hr and infiltrated overnight in a 1:1 mixture of propyleneoxide and TAAB
249 (TAAB Laboratories Equipment Ltd). The following day the samples were embedded in TAAB
250 Epon and polymerized at 60ºC for 48 hrs. Ultrathin ~60 nm sections) were cut on a Reichert
251 Ultracut-S microtome, picked up on to copper grids stained with lead citrate and examined in a
252 JEOL 1200EX Transmission electron microscope and images were recorded with an AMT 2k
253 CCD camera.
254

255 **2.7 Phylogenetic analysis.**

256 The following 18S rRNA gene sequences were used: *Cryptosporidium parvum* (GenBank
257 accession no.: L25642.1), *Cryptosporidium muris* (AB089284.1), *Babesia bovis* (L19077.1),
258 *Babesia bigemina* (JQ437261.1), *Babesia divergens* (AJ439713.1), *Babesia duncani*
259 (HQ285838.1), *Babesia microti* (AB219802.1), *Theileria annulata* (EU083801.1), *Theileria*
260 *parva* (L02366.1), *Theileria orientalis* (HM538200.1), *Cytauxzoon felis* (L19080.1), *Theileria*
261 *equi* (KM046918.1), *Hepatozoon canis* (KX712124.1), *Plasmodium falciparum*

262 (XR_002966654.1), *Plasmodium berghei* (XR_002688202.1), *Plasmodium vivax*
263 (XR_003001225.1), *Toxoplasma gondii* (L24381.1), *Hammondia hammondi* (KT184369.1),
264 *Neospora caninum* (U03069.1), *Besnoitia besnoiti* (KJ746531.1), *Cystoisospora suis*
265 (KF854251.1), *Sarcocystis neurona* (KT184371.1), *Hyaloklossia lieberkuehni* (AF298623.1),
266 *Goussia janae* (GU479644.1), *Goussia neglecta* (FJ009242.1), *Cyclospora cayetanensis*
267 (XR_003297358.1), *Eimeria callospermophili* (JQ993648.1), *Eimeria tenella* (KT184354.1),
268 *Eimeria necatrix* (KT184349.1), *Eimeria maxima* (KT184346.1), *Eimeria brunetti*
269 (KT184337.1), and *Eimeria acervulina* (KT184333.1). Sequences were aligned using Clustal
270 Omega (Sievers et al., 2011) and a consensus phylogenetic tree was generated using Geneious
271 Prime V2019.1.3 (Invitrogen) using the Jukes-Cantor genetic distance model, neighbor-joining
272 tree build method, bootstrapped 100x using *C. parvum* as outgroup.
273

274 **2.8 Generation of *B. bigemima* IMC1a antiserum**

275 We identified five *B. bigemina* IMC proteins by reciprocal BLASTP searches on EuPathDB
276 (Warrenfeltz et al., 2018) with the 14 *T. gondii* alveolin-domain containing IMC proteins
277 (Anderson-White et al., 2011): PiroplasmaDB.org accession number BBBOND_0204530,
278 BBBOND_0401990, BBBOND_0201220, BBBOND_0208040, BBBOND_0300730). *B.*
279 *bigemina* BBBOND_0204530, which we named BbIMC1a, was most conserved and the whole
280 ORF of 600 bp was synthesized by TwistBioscience (San Francisco, CA), amplified with
281 primers #4831 pAVA-Gibson-Twist-F gaagctcagacccaggg and #4832 pAVA-Gibson-Twist-R
282 tgcagaacttgttcgtgctg to remove the linkers and cloned by Gibson assembly into *Pme*I/*Nru*I
283 digested plasmid pAVA0421 (Alexandrov et al., 2004), expressed as a 6-His tag fusion in
284 *Escherichia coli* BL21-RIPL, purified by Ni-NTA chromatography under denaturing conditions
285 (Invitrogen), refolded, and used to immunize a guinea pig (Covance, Inc). Serum was affinity
286 purified as described previously (Gubbels et al., 2006) against recombinant His6-BbIMC1a.
287

288 **3 Results**

289 **3.1 External budding**

290 Schizogony is defined as: schizo = split (or cleft); gony = birth (genesis of a class of thing). It is
291 generally understood as meaning “multi-fission” and is applied to division modes producing
292 more than two daughter cells per division by peripheral (or cortical) budding from the plasma

293 membrane of a polyploid, multi-nucleated mother cell (Fig 2). However, confusion enters with
294 the term "schizont", which is more widely defined and used to describe any polyploid
295 intermediate cell state regardless of division mode (Fig 4-6): schizo = split (or cleft); -ont = a
296 being (from Greek einai to be) i.e., "to be split". We forewarn that the term 'schizont' is and will
297 be used across division modes for polyploid cells, and thus will not always refer to schizogony
298 per se.
299

300 **3.1.1 Schizogony with karyokinesis**

301 A wide array of Apicomplexa impacting humans or livestock divide by schizogony, such as
302 nearly all Eimeriidae family members of the Coccidian parasites (Dubremetz, 1973; Joyner and
303 Long, 1974; Dubremetz and Elsner, 1979; Ferguson et al., 2008), the genus of *Plasmodium* in the
304 order of Haemosporida (Arnot et al., 2011; Stanway et al., 2011) as well most (but not all!)
305 piroplasms compromising *Theileria* and *Babesia* spp. (Mehlhorn and Shein, 1984) (Fig 1). The
306 piroplasms are tick-transmitted parasites that multiply in red blood cells without forming
307 pigments (order Achromatorida). Both the piroplasms and the *Plasmodium* spp. (order
308 Chromatorida: form pigments in red blood cells) reside in the clade Haemosporidia for their
309 shared residence within red blood cells. Our discussion here is based mostly on *Plasmodium*
310 schizogony in the red blood cells as it is best studied system, however, insights likely apply
311 widely. A defining principle of schizogony is the disassembly of the mother's cytoskeleton
312 shortly following completion of host cell invasion, resulting in an amoeboid or pleomorphic cell
313 (Hepler et al., 1966; Gruring et al., 2011) (Fig 2A2) which then undergoes several cycles of
314 DNA replication and nuclear division (Fig 2A3,4). These rounds of DNA replication without
315 budding are controlled by cdc2-related kinase CRK4 which resides in the nucleoplasm and is
316 associated with phosphorylation of the DNA replication machinery (Ganter et al., 2017).
317 Interestingly, the mitotic cycles of the nuclei sharing the same cytoplasm are not synchronous.
318 Mechanistically, this observation is anchored in a differential maturation model of mother and
319 daughter centrosomes following their duplication. Although this model has been firmly
320 demonstrated in higher eukaryotes and is defined by proteins in the centrosome's distal and sub-
321 distal appendages (Bornens and Gonczy, 2014), it has not been formally confirmed in the
322 Apicomplexa. The last cycle of S/M-phase, in contrast, is synchronous and coupled to the
323 synchronous budding of the daughters at the end of schizogony (Ferguson et al., 2008; Kono et

324 al., 2016; Rudlaff et al., 2019) (Fig 2A4,5). Budding follows the activation of the centrosomes'
325 outer-cores, which is always tied to simultaneous centrosome inner-core activation. The exact
326 timing of the nuclear cycle before the onset of budding has not been clearly resolved. Notably,
327 the level of PfCRK4 drops when the budding cycle is about to start, but it is not clear whether
328 this is the defining signal synchronizing the nuclear cycles and/or activating the budding cycle.
329 Potentially, a diffusible signaling protein could respond to the depletion of nutrients, the
330 accumulation of waste, limited space, or act as a quorum sensor, and subsequently synchronize
331 or halt the nuclear cycle before activating the synchronous budding phase. Since the number of
332 offspring varies across *Plasmodium* species, even between different *P. falciparum* strains, across
333 different development stages (e.g. the liver cell expands and produces up to 90,000 merozoites
334 from infection by a single sporozoite (Vaughan and Kappe, 2017)) there is also a strong,
335 programmed genetic component determining the number of offspring (Reilly et al., 2007). Either
336 way, when the 'commitment to budding' checkpoint is cleared, the centrosomes that anchor the
337 spindle pole and chromosomes, reorient to associate with the plasma membrane, a step which is
338 mediated by Cyc1 (Robbins et al., 2017). Note that the centrosomes in *Plasmodium* spp.
339 technically are centriolar plaques as these parasites lack canonical centriolar structures.
340 Following plasma membrane docking of the centrosomes, the daughter cytoskeletons start to
341 assemble in connection with the plasma membrane and the buds move outward (Fig 2A4,5). In
342 *P. falciparum* the maturation and release of daughters is mediated by CINCH, a contractile
343 protein in the basal complex (Rudlaff et al., 2019).
344

345 **3.1.2 Schizogony with limited karyokinesis**

346 Although not separately recognized in the naming conventions, a variation on the classical
347 schizogony as described in the preceding section occurs during sporozoite formation in the
348 invertebrate vector wherein sexual development takes place (Fig 1). This happens in the
349 mosquito midgut for the *Plasmodium* spp (Simonetti, 1996) and in the tick salivary gland for
350 most piroplasms, including *Theileria* spp. and many *Babesia* spp. (Mehlhorn and Shein, 1984;
351 Jalovecka et al., 2018). *P. berghei* and *P. falciparum* sporogenesis have been most extensively
352 studied, which occurs in an extracellular oocyst residing under the basal lamina of the midgut
353 wall (Simonetti, 1996). Like in classical schizogony, the mother's cytoskeleton is disassembled
354 resulting in a pleomorphic cell. Here, DNA replication and mitosis are not always followed by

355 karyokinesis leading to a patchwork of nuclei, with varying levels of ploidity (Fig 2B). Again,
356 the individual nuclei are at different levels of S-phase and mitosis, however, within one
357 polyploid nucleus this cycle is largely synchronous (Howells and Davies, 1971b; a; Schrevel et
358 al., 1977; Sinden and Strong, 1978). Typically, a round of sporogenesis produces thousands of
359 individual sporozoites from a single mother cell. Similar to classical schizogony, the budding of
360 daughters from the cortex occurs simultaneously and is coupled to a synchronized round of S-
361 phase and mitosis (Howells and Davies, 1971a; Schrevel et al., 1977; Araki et al., 2019; Pandey
362 et al., 2019). This process is conserved in *Theileria* and *Babesia* spp. as well, where multiple and
363 multi-lobed nuclei are especially prominent (Moltmann et al., 1983). However, some *Babesia*
364 spp., produce sporozoites through binary fission (Mehlhorn and Shein, 1984).
365 In summary, the intriguing phenomenon is that karyokinesis seems to be optional in these
366 polyploid schizonts. The synchronized cycles of mitosis within a single nucleus suggest that
367 mitotic cycles are organized on the nucleoplasm level just as in classical schizogony, whereas
368 commitment to budding is a factor shared across the whole cytoplasm. How these events are
369 controlled at the molecular level has not been determined.
370

371 **3.1.3 Binary and multiple fission**

372 Binary fission is defined as "the formation of two daughter cells per division round". Among the
373 Apicomplexa, binary fission is used to describe the division process in the red blood cell stages
374 of many *Babesia* and *Theileria* parasites. Most *Babesia* spp. form two daughters per division
375 round, i.e. classical binary fission. However, in the red blood cell cycle several clades of
376 *Babesia*, including *Babesia duncani* (Conrad et al., 2006) and *B. microti* (Rudzinska, 1981),
377 form four merozoites per division round (Maltese cross), as do all *Theileria* spp. (Conrad et al.,
378 1985; Conrad et al., 1986; Fawcett et al., 1987; Uilenberg, 2006). This process is known as both
379 schizogony and 'multiple fission', however it is generally considered distinct from schizogony,
380 which as mentioned above, is a term historically used when many more daughters are produced.
381 The term "binary fission" does not imply that budding is involved and does not intuitively
382 connect with "multiple fission", which produces only four daughters per division round, as
383 defined in schizogony. Due to the lack of clarity on how these processes are related and defined
384 cell biologically, the exact nature of *Babesia* cell division in the red blood cell remains to be
385 elucidated. The ambiguity of the used terms (i.e. binary fission, budding, schizogony) to describe

386 this process further exacerbates this confusion. In a 1978 publication study using transmission
387 electron microscopy (TEM) the interpretation was as follows (Potgieter and Els, 1977): "The
388 trophozoites were surrounded by a single membrane, were pleomorphic in shape and contained
389 large inclusions of host cell cytoplasm, but no cytostomes or food vacuoles could be identified.
390 Reproduction took place through a process resembling schizogony resulting in the production of
391 two merozoites, the cytoplasmic constituents of the original trophozoite (mother cell) being
392 virtually entirely incorporated into the daughter cells in the process". In essence, the
393 pleomorphic/ameboid trophozoite in combination with the schizogony reference suggest that the
394 process is conceptually very similar to schizogony, except that term does not capture it since
395 only two daughters are formed. Here we combine existing data with new insights from *in vitro*
396 cultivated *Babesia bigemina* to clarify the mechanistic murkiness surrounding binary fission.
397 *B. bigemina* is a cattle-infecting, tick-transmitted apicomplexan causing vast economic losses
398 (Bock et al., 2004; Suarez et al., 2019). From an experimental point of view, *B. bigemina* cell
399 division is uncomplicated in that it only produces two daughters per division round, and it is a
400 relatively large *Babesia* spp., making it an ideal candidate for microscopy. We focused on the
401 key organizers of cell division: the centrosome (or centriolar plaques) and cortical cytoskeleton.
402 *T. gondii* Centrin1 antiserum on *B. bigemina* showed a specific, albeit relatively weak, signal,
403 but only during daughter budding (Fig 3A). It therefore appears that centrosome composition is
404 dynamic, which was recently also reported for *P. berghei* Centrin4 as this signal was only on the
405 centrosome during mitosis and budding, but not in mature or recently invaded parasites (Roques
406 et al., 2019). In contrast, *Plasmodium* Centrin3 is a popular marker of centrosomes and is always
407 associated with the centrosome, indicating that the dynamics of different Centrins can vary
408 (Mahajan et al., 2008; Kono et al., 2012). We detected microtubules with α-tubulin MAb 12G10
409 generated against ciliate *Tetrahymena thermophila* (Jerka-Dziadosz and Frankel, 1995), which
410 has shown broad reactivity in the Apicomplexa. A spot focused toward the apical end was
411 observed (Fig 3A), but we never observed tubulin in the nucleus, suggesting this antibody does
412 not detect the mitotic spindle. In *Plasmodium* the spindle was successfully visualized with
413 monoclonal antibody B-5-2-1 generated against sea urchin α-tubulin (Gerald et al., 2011), but in
414 *B. bigemina* we observed the same patterns as for MAb 12G10 (not shown). In *T. gondii*,
415 detecting the spindle microtubules has also been challenging, but a polyclonal serum against
416 TgEB1, a microtubule (+)-end binding protein, was very specific for the spindle (Chen et al.,

417 2015b). Reactivity of α-TgEB1 in *B. bigemina* across all parasite stages highlighted a spot basal
418 of the apical tubulin staining (Fig 3B). We interpret that EB1 does not bind to the spindle
419 microtubules in *B. bigemina*, but instead associates with the (+)-end of the subpellicular
420 microtubules emanating from the MTOC at the very apical end. This also indicates these
421 microtubules are relatively short and only cover the very apical cap of the parasite. To better
422 visualize the cortical cytoskeletal scaffolds that drive budding we tested polyclonal antisera
423 generated against *T. gondii* IMC proteins (Gubbels et al., 2004; Anderson-White et al., 2011),
424 but unfortunately none showed a signal. Therefore, we generated a specific *B. bigemina* IMC
425 antiserum against BBBOND_0204530, the closest relative to the *T. gondii* alveolin domain
426 containing IMC proteins (Anderson-White et al., 2011), which we named BbIMC1a (Fig S1).
427 IFAs with α-PbIMC1a nicely highlighted the cortical cytoskeleton during budding, extending
428 basally beyond the microtubule signal. In mature parasites we observed signal along the entire
429 length of the merozoite (Fig 3C). In trophozoites we also observed parasites identified by their
430 DAPI signal with weak or variable intensities of either the IMC1a or tubulin signals that
431 appeared disorganized, or at least not to outline a merozoite (Fig 3C top panel and middle panel
432 marked by an asterisk). We interpreted these amorphic signals to represent trophozoites that are
433 at the stage between invasion and the start of cell division. However, across all parasites in
434 division we observed parasites forming next to each other, with apical ends emerging first with
435 V-shape symmetry.
436 To obtain a higher resolution of the mechanistic steps in the *B. bigemina* division process we
437 performed TEM. We focused on stages after the parasites escaped from their vacuole and entered
438 G1 growth phase (trophozoites). We observed a high frequency of zoites wherein the IMC
439 breaks into 5-6 pieces, still in curved structures on the edge consistent with an ameboid or
440 pleomorphic status for the zoites (Fig 3D1). This consistent observation suggests that
441 disassembly of the mother cytoskeleton is spatially organized resulting in a symmetrical
442 appearance, which reflect the trophozoites identified by IFA (Fig 3C). Similar observation on
443 disassembling mother IMC have been reported for *Plasmodium* ookinetes in the mosquito
444 midgut (Carter et al., 2007), and for sporozoites in liver cells, where regularly spaced breaks
445 occur in the IMC, although not quite as symmetrically organized as seen here in *B. bigemina*
446 (Jayabalasingham et al., 2010). In a budding zoite two daughter buds are emerging on one side of
447 the cell (like rabbit ears), and not on polar opposites (Fig 3D2). The shape of the nucleus is also

448 consistent with the anchoring of the nucleus at the apical end of the daughters, which, by using
449 other division modes as a guide, we assume is through the spindle poles (Potgieter and Els,
450 1977). For the growing stages, we captured many transverse cross sections of two side-by-side
451 budding daughters with the nucleus at various stages of division (Fig 3D 3-5). Finally,
452 completely formed daughters appear side by side under a similar angle as the early daughter buds
453 (compare the orange arrows in Fig 3D2 with 3D6). Additional TEM images of *Babesia* buds in a
454 V orientation consistent with our data have been reported elsewhere (Friedhoff and Scholtyseck,
455 1977; Potgieter and Els, 1977; Scholtyseck, 1979). A section through the basal ends of still
456 connected *Babesia divergens* parasites (predominantly a cattle parasite but opportunistic in
457 humans) displays an electron dense structure on the basal end of the IMC consistent with a basal
458 complex (Fig 3E). Although we did not capture a section through this structure in *B. bigemina*, a
459 similar appearance of the basal complex in *B. bigemina* has been reported previously (Potgieter
460 and Els, 1977).
461 Overall, the budding of daughters in *B. bigemina* shares many features seen across asexual
462 apicomplexan development (Fig 3F). First, the angle between the daughter buds fits with the
463 pleuromitosis (closed mitosis with the spindle poles in close proximity at one side of the nucleus)
464 model dictated by closely apposed centrosomes at the apically defining side of the nucleus. This
465 is observed across the Apicomplexa that have been studied (Gerald et al., 2011; Francia and
466 Striepen, 2014). As a result, daughter buds are formed next to each other rather than in opposing
467 orientations (middle panel Fig 3F3-5). The *B. bigemina* trophozoite has an ameboid appearance
468 after invasion and cytoskeleton is disassembled (Fig 3E1, 3F2; and (Potgieter and Els, 1977)),
469 which likewise is observed during the corresponding stage of *P. falciparum* (Gruring et al.,
470 2011). Taken together, these data firmly illustrate that the processes known as binary fission and
471 schizogony, and by extension multiple fission as seen in *Theileria* spp., are mechanistically the
472 same and only differ in the number of nuclear replication cycles before the onset of cytokinesis.
473 Collectively, we now group these division forms together under the umbrella "external (aka
474 cortical) budding"
475
476 **3.1.3 Other variations on cortical budding**
477 Schizogony by cortical budding as described in the preceding sections are found in various
478 asexual stages. Other forms on cortical budding can be found in sexual development stages,

479 which we will briefly highlight here to illustrate the spectrum of division modes. *Plasmodium*
480 male gametocytogenesis produces flagellated microgametes in a process known as
481 "exflagellation". This process occurs in the red blood cell and unfolds by several fast rounds of
482 S/M-phase resulting in a single polyploid nucleus (Sinden et al., 1978; Sinden, 1983). The
483 cortical 'budding' of microgametes, which at the cytoskeletal level basically are a single
484 flagellum and only contain microtubules, progresses while the nuclear material partitions.
485 Interestingly, a recent study using Ndc80 as a marker for the kinetochores demonstrated that the
486 genome size universally increases to 8N, but that chromosome replication is asynchronous
487 (Pandey et al., 2019). This is in contrast to what is observed during asexual schizogony, where
488 the rule is that the mitotic cycles are synchronous within a shared nucleoplasm.
489 In addition, microgametocyte formation of *T. gondii* also progresses through a cortical
490 budding process (Ferguson et al., 1974). As discussed in detail below, it is salient to note that the
491 asexual division of *T. gondii* is by internal budding, not through cortical budding. *T. gondii*
492 microgametocytes formation plays out by the association of 1N nuclei in a multi-nucleated
493 microgamont with plasma membrane of the mother cell. Interestingly, the mother cell
494 (macrogamont) maintains an IMC where in holes are present to facilitate association of the
495 nuclei with the plasma membrane. From here, bi-flagellated microgametes bud outward in a
496 cortical budding process (Ferguson et al., 2008). Interestingly, this process is conserved across
497 the Coccidia, as it is also reported for *Eimeria* spp. which, in contrast to *T. gondii*, replicate
498 asexually by schizogony (Ferguson et al., 1980) (Fig 1). Taken together, the notable features here
499 are maintenance of the cortical cytoskeleton (Dubey et al., 2017) in combination with cortical
500 budding while S-phase, mitosis and karyokinesis have been completed before the onset
501 'budding'.
502

503 **3.2 Internal budding**

504 **3.2.1 Endodyogeny**

505 Endodyogeny is defined as: endo = inner/internal; dyo = two; geny = genesis, meaning birth;
506 production/generation/origin. This term is applied to a type of reproduction in which two
507 daughters are formed within a parent cell (Goldman et al., 1958; Sheffield and Melton, 1968).
508 Endodyogeny has been described in detail for *T. gondii* tachyzoites (Nishi et al., 2008;
509 Anderson-White et al., 2012) and is employed as well by its closest evolutionary neighbors

510 comprising several genera of the Sarcocystidae (Fig 1, 4). These include *Hammondia*, *Neospora*
511 and *Besnotia* spp. as well as the tissue cyst-forming stages of *Sarcocystis neurona.* During
512 endodyogeny, the mother's cytoskeleton is not disassembled following completion of invasion,
513 and two daughter buds assemble on centrosomes residing within the cytoplasm. Only at the very
514 last stage of daughter budding is the mother's cytoskeleton disassembled and is the plasma
515 membrane deposited on the new daughters, which is mediated by recruitment of the "gliding
516 motor complex" to the IMC. This complex contains a multi-acylated protein glideosome
517 associated protein, GAP45, that is anchored in both the plasma membrane and the IMC outer
518 membrane and 'zippers' these structures together in an apical to basal direction (Gaskins et al.,
519 2004; Frenal et al., 2014). Many of the cell cycle checkpoints throughout endodyogeny have
520 been resolved. Specifically, two checkpoints have been described upon commitment to mitosis
521 and budding, one likely dedicated to mitosis and the other to budding. This is thought to facilitate
522 the uncoupling of S/M cycles from budding in the multi-daughter division modes and
523 differentially activate the centrosome inner- and outer-cores (Suvorova et al., 2015; Naumov et
524 al., 2017; White and Suvorova, 2018). Like in schizogony, daughter budding occurs in sync with
525 S/M-phase and karyokinesis. Upon emergence of daughters, a narrow cytoplasmic bridge at the
526 basal end remains connected with a residual body containing remnants of the mother cell, which
527 will be largely resorbed into the daughters (Frenal et al., 2017b; Periz et al., 2019). As a result,
528 the daughter parasites remain in contact with each other and could therefore have the false
529 appearance of endopolygeny. To differentiate these two processes, this division process has been
530 referred to as 'repeated endodyogeny'.
531

532 **3.2.3 Endopolygeny**

533 Endopolygeny is defined as: endo = inner/internal; poly = multiple; geny= genesis/birth. This
534 term is used to describe the reproduction types wherein more than two individuals are formed
535 simultaneously within the cytoplasm (i.e. not from the cortical periphery) of a polyploid parent
536 cell. One of the key features of internal budding is that the mother's cytoskeleton is maintained
537 throughout cell division and only dissembles just before the emergence of almost completely
538 assembled daughters. Although not differentiated in the naming conventions, two sub-forms can
539 be distinguished: either the polyploid mother cell can be multinucleate, or it can contain one
540 large polyploid nucleus depending on whether karyokinesis follows each round of S-phase. Both

541 these forms of budding are found within the tissue cyst-forming Coccidia, more specifically the
542 Sarcocystidae (Fig 1, 5, 6). These division forms are related to endodyogeny, since the mother's
543 cytoskeleton is maintained throughout the division cycle until the maturation of the daughter
544 cells. We define these three forms here collectively as "internal budding". Internal budding by
545 the Sarcocystidae is unique among the Coccidia as other families, notably the closely related
546 Eimeriidae, replicate by schizogony (Fig 1). Two emerging systems exist to study the variations
547 in progression of endopolygeny: *Sarcocystis neurona* is a model for studies representing the
548 form without completing karyokinesis (Fig 5) (Vaishnava et al., 2005; Dubey et al., 2017),
549 whereas merogony of *Cystoisospora suis* provides an accessible *in vitro* model for the form
550 including karyokinesis after each S/M-round (Fig 6) (Worliczek et al., 2013).
551
552 **3.2.3.1 Endopolygeny with karyokinesis**
553 *C. suis* is the causative agent of suckling piglet coccidiosis (Shrestha et al., 2015). Although
554 phylogenetically *C. suis* falls within the cyst-forming Coccidia (Fig 1), tissue cysts have never
555 been observed and the known coccidian development cycle is monoxenic in pigs: the absence of
556 tissue cyst forming capacity is likely a secondary loss in this species (Stuart et al., 1982; Shrestha
557 et al., 2015). *C. suis* asexually replicates in epithelial cells of the porcine small intestine by
558 endodyogeny and endopolygeny, depending on the generation of asexual stages (alternatively
559 called types: meronts/merozoites type I, II and subtype II (Matuschka and Heydorn, 1980). Early
560 asexual division after infection of the gut epithelium is restricted to endodyogeny (often in
561 consecutive cycles within one parasitophorous vacuole, i.e. 'repeated endodyogeny'), whereas
562 endopolygeny is described from day 3-4 post infection onwards *in vivo* (Lindsay et al., 1980;
563 Matuschka and Heydorn, 1980) and from day 7 onward *in vitro* (Worliczek et al., 2013),
564 concurrent with cells replicating by endodyogeny.
565 As for *B. bigemina*, we tracked *in vitro* progression of *C. suis* development using the
566 toolbox of reagents we established for *T. gondii*. In *C. suis* zoites undergoing endopolygeny, the
567 mother's subpellicular microtubule cytoskeleton is clearly visible in large polyploid cells as an
568 apically concentrated microtubular accumulation joined in the mother's conoid (Fig 5A-D). This
569 confirms the mother's cytoskeleton is maintained throughout endopolygeny. To track the
570 progression of S/M-phase across the nuclei we used the kinetochore component Nuf2 (Farrell
571 and Gubbels, 2014) in combination with acetylated α-tubulin, which marks the spindle poles

572 during mitosis (note that spindle microtubules disassemble during interphase (Farrell and
573 Gubbels, 2014; Chen et al., 2015b)). The first observation is that the status of mitosis (spindle
574 visible by tubulin stain) and the status of kinetochore separation varies among nuclei within the
575 same cell (Fig 5A, B). Furthermore, it is evident that parasites expand non-geometrically, as
576 counted by spindle poles per nucleus varying from 3, 4, 5, to 6 are seen in Fig 5A and B, whereas
577 12 budding daughters, i.e. non-geometrically expanded, can be discerned in Fig 5C, D. These
578 two observations indicate that the nuclear division cycles are not synchronous, which is
579 consistent with expansion numbers described in the literature (e.g. (Lindsay et al., 1980;
580 Matuschka and Heydorn, 1980)). Here we show for the first time that this is associated with
581 asynchronous nuclear replication cycles. Finally, we show that the final round of mitosis is
582 synchronous for all nuclei and is coupled with daughter budding, as seen in schizogony. Our
583 insights are summarized in the schematic of Fig 5E. Based on the details revealed here, we
584 conclude that like in schizogony, the S/M-phase progression are controlled at the nuclear level,
585 most likely differing maturity of the mother and daughter centrosomes, but that the commitment
586 to budding is synchronized across the cytoplasm.
587 Reports on *T. gondii* endopolygeny suggest geometric expansion of nuclei: 8–16 progeny per
588 endopolygeny replication cycle in the cat gut have been observed (Ferguson et al., 1974).
589 Historically, the sexual cycle of *T. gondii* has been poorly experimentally accessible, but *in vitro*
590 completion of the sexual cycle in cat intestinal organoids was recently reported, which is
591 expected to provide experimental accessibility (Martorelli Di Genova et al., 2019). To date, *T.*
592 *gondii* endopolygeny studies have not been so comprehensive to support a strong conclusion in
593 this matter.
594 An additional notable observation in Fig 5A is the presence of multiple parasites within a
595 single vacuole undergoing endopolygeny. It has been described before that several multinucleate
596 meronts can be present in a single vacuole, which indicates that more than one asexual division
597 occurs in the same cell (Lindsay et al., 1980). As such, this reveals that multiple rounds of
598 budding within the same vacuole are not exclusively found during endodyogeny as described
599 above for *T. gondii*. This phenomenon therefore highlights that the timing of budding is
600 determined by a genetic program, and not controlled by environmental factors, which we also
601 concluded for schizogony.
602

603 **3.2.3.1 Endopolygeny without karyokinesis**

604 *S. neurona* has a sylvatic cycle in the Americas with small mammals as intermediate hosts and
605 the opossum as the definitive host. However, accidental infection of horses can cause equine
606 protozoal myeloencephalitis (EPM) (Reed et al., 2016). Using the same strategy as mentioned
607 above, we observe an apical concentration of microtubules across cells with progressively larger
608 single nuclei indicating the mother's cytoskeleton is maintained throughout endopolygeny
609 (arrowheads in Fig 6A). Furthermore, the *S. neurona* IMC can be visualized through
610 overexpression of TgIMC15-YFP, which highlights the sutures in the IMC of the mother
611 throughout development (Fig 6B) (Dubey et al., 2016). When the cell prepares for budding
612 IMC15 also appears on the centrosomes at which point the mother's IMC is still prominently
613 present (Fig 6B2). Only at the conclusion of the budding process is the mother's cytoskeleton
614 disassembled, which mimics the dynamics of the IMC during *T. gondii* endodyogeny (Anderson-
615 White et al., 2011; Dubey et al., 2016).

616 In contrast, to *C. suis*, the S/M cycles of *S. neurona* are completely synchronized: in Fig 6A2
617 we observe a cell in interphase characterized by absence of spindle microtubules, whereas the
618 right cell displays spindle microtubules associated with each centrosome. This confirms previous
619 observations (Vaishnava et al., 2005), and indicates that when the nucleoplasm is shared, the
620 individual status of centrosome maturation is overruled, likely by a factor diffusing in the
621 nucleoplasm. Late in development the large polyploid 32N nucleus shifts into a multi-lobed,
622 'serpentine' morphology (Fig 6A3), which sets the stage for a final round of S/M-phase now
623 coupled to karyokinesis and internal budding resulting in 64 daughters (Fig 6A4). Thus, when
624 the S/M-phase are not followed by karyokinesis the nuclear cycles remain synchronized and
625 progeny number are the result of geometric expansion.

626

627 **3.2.4 Budding without multiplication and multiplication without budding**

628 The spectrum of division modes not yet covered spans two more manifestations in sexual
629 development stages. The first, budding without multiplication, is the formation of kinetes in the
630 Heamosporidia. The *Plasmodium* spp. generate ookinetes from a fertilized zygote (ploidity of 2-
631 4N in a single nucleus) that cross the mosquito gut wall (reviewed in (Angrisano et al., 2012;
632 Bennink et al., 2016)). Although the zygote lacks a cortical cytoskeleton, the ookinete has a
633 complete cortical cytoskeleton comprising IMC and cortical microtubules. This cortical

634 cytoskeleton is formed by the ookinete through from the cortex of the zygote in absence of
635 karyokinesis, though a budding stage dubbed 'retort' (Canning and Sinden, 1973; Carter et al.,
636 2007). Yet even more exotic variations occur in the piroplasms; both *Theileria* and *Babesia* spp.
637 produce kinetes, which do not bud from the cortex, but into an internal vacuole formed inside the
638 zygote (see (Mehlhorn and Shein, 1984) for a detailed review). Thus, cortical budding can be
639 uncoupled from the nuclear cycle in the zygote stages.

640 The second variation is multiplication without budding, of which there are three different,
641 possibly related examples. The first is found in the *Babesia* spp. kinetes, which following their
642 formation in the tick gut, cross the midgut and migrate to the tick ovary. Here, the cortical
643 cytoskeleton disassembles and the cell transforms into a pleomorphic cell (Moltmann et al.,
644 1982; Mehlhorn and Shein, 1984). Subsequently, several rounds of S/M-phase without
645 karyokinesis occur to produce a multiploid, lobed nucleus. In a process not understood at neither
646 the mechanistic nor molecular level, these large cells divide into multiple cells, each with a
647 single nucleus. Surprisingly, neither the mother nor the daughter cells have a cortical
648 cytoskeleton. This indicates that at this life stage cell division is independent of any form of
649 budding, and thus indicates that in Apicomplexa the cortical cytoskeleton is not a strict
650 requirement for cell division. From each of these pleomorphic cells a new kinete then forms by
651 budding mediated by cortical cytoskeleton formation into an internal vacuole as described above.
652 The released kinetes then migrate to the salivary glands where they undergo sporogenesis.

653 The second example of multiplication without budding is a binary variation on the above
654 process found in some *Babesia* spp. (Mehlhorn and Shein, 1984). Kinetes that invaded the tick
655 salivary gland disassemble their cytoskeleton and undergo one round of S/M-phase, karyokinesis
656 and cell division. However, no cortical cytoskeleton is assembled during these binary division
657 rounds. The cortical cytoskeleton is reportedly assembled slowly during the last couple of
658 division rounds resulting in mature sporozoites. Thus, the salient details are that this process is
659 binary and appears to be efficient with resources as the cytoskeleton is only assembled in the last
660 round (unlike endodyogeny, where a complete parasite is assembled each multiplication round).
661 This process has been described for *B. canis* (Schein et al., 1979), a dog parasite, and *B. bovis*
662 (Potgieter and Els, 1976), a cattle parasite, but likely occurs widely across *Babesia* spp.
663 exclusively replicating by binary fission in the red blood cell (Fig 1) (Mehlhorn and Shein,
664 1984). Thus, across all life stages, these particular *Babesia* parasites seem to have lost the ability

665 to produce more than two daughters per division round, providing a model system to unravel the
666 specifics of the genetic program and regulatory network.
667 The third example is the process of sporoblast formation in the Coccidia. This occurs within
668 the oocysts released into the environment. Depending on the species, the zygotes can divide
669 themselves into 2 to 4 sporoblasts (this number is a defining feature in diagnosis of fecal oocysts;
670 not dividing is an option as well (Gardiner et al., 1998)). Inside the sporoblasts 2-4 sporozoites
671 form through a budding mechanism coupled to DNA replication. Although studied in many
672 parasites, *T. gondii* produces two sporoblasts and four sporozoites per sporoblast and as such is
673 the simplest form. Consistent with EM data (Ferguson et al., 1979a), it was recently shown that
674 neither microtubules nor IMC proteins were involved in *T. gondii* sporoblast formation (Dubey
675 et al., 2016). Considering the process and life stage, this process therefore appears akin to kinete
676 multiplication in *Babesia* spp., as described above. This thus seems to connect these two
677 parasites across a large phylogenetic distance, which begs the question whether this is an
678 ancestral connection, or a case of convergent evolution.
679

680 **4. Discussion**

681 The picture of cell division across all life stages of the Apicomplexa is that principle differences
682 exist between the sexual and asexual cell division strategies. In the sexual stages, cell number
683 expansion is not necessarily related to budding a daughter cytoskeleton. This shows that budding
684 is in principle not required for apicomplexan cell division, but there are very few mechanistical
685 or molecular details available for these division modes. The other insight is that all invasive
686 zoites with an apical complex form by a budding strategy, which is initiated and coordinated by
687 the centrosome's outer-core and proceeds in an apical to basal assembly direction. In all the
688 asexual life cycle stages zoite budding is coupled to a complete nuclear cycle (S/M-phase plus
689 karyokinesis). Another general rule across asexual development is that budding is synchronized
690 across the whole cell. This indicates that the centrosome outer-core activation is always coupled
691 to inner-core activation in asexual stages on a shared cytoplasm-wide level (e.g. a diffusible
692 kinase or kinase substrate). The exceptions to this rule are only found in sexual stages:
693 microgametocytogenesis and (oo)kinete formation in the Haemosproridia.
694 Besides these general rules, there are several variations within asexual division modes which
695 partition into two mechanistically different strategies: internal budding and external budding (Fig

696 1). Internal budding comprises endodyogeny and the two variations on endopolygeny, whereas
697 external budding captures the two variations on schizogony, binary fission, and multiple fission.
698 The number of offspring in each strategy can vary from two (endodyogeny and binary fission) to
699 several orders of magnitude higher (>10,000 in schizogony). At the furthest extreme are several
700 bovine-infecting *Theileria* spp. of which the schizonts in the white bloods that trigger
701 transformation of their lymphocyte host cells (i.e. leukemia) resulting in division and expansion
702 of the parasites schizont stage along with their host cell (Luder et al., 2009; Chakraborty et al.,
703 2017). As remarked throughout, the number of daughter cells per division round in each life
704 stage is largely genetically controlled, but the details on the controls are just starting to emerge.
705 Overlapping with the genetic switch committing to budding is the bi-partite centrosome
706 cycle. The apicomplexan centrosome and mitotic cycles are controlled by Nek and Aurora
707 kinases (Reininger et al., 2011; Carvalho et al., 2013; Chen and Gubbels, 2013; Berry et al.,
708 2016; Berry et al., 2018). In *T. gondii* it has been demonstrated that the switch from solely a
709 nuclear cycle to a combined nuclear and budding cycle is controlled by a MAP kinase-like
710 protein (Brown et al., 2014; Sugi et al., 2015; Suvorova et al., 2015). Ultimately, cell cycle
711 progression and the activation of each core is regulated by cyclin and CDK pairs adapted to each
712 apicomplexan cycle, as they likely act independently on the inner- and outer-centrosome cores
713 (Le Roch et al., 2000; Merckx et al., 2003; Alvarez and Suvorova, 2017; Ganter et al., 2017;
714 Naumov et al., 2017; Robbins et al., 2017; White and Suvorova, 2018). An open question is the
715 identity on the factor(s) controlling the pause of nuclear cycles across parasites prior to the final
716 round of coupled S/M-phase and budding in the polynucleate division modes.
717 The control of the nuclear cycle appears to depend on the ploidy of the nucleoplasm. When
718 each S/M-phase is followed by karyokinesis, then the cycles of individual nuclei are diverging.
719 Mechanistically, this observation is anchored in differential maturation of mother and daughter
720 centrosomes following their duplication; the mother centrosome is sooner primed for another
721 round of replication. This mechanism has been firmly demonstrated in higher eukaryotes and is
722 defined by proteins in the centrosome's distal and sub-distal appendages (Bornens and Gonczy,
723 2014). However, this has not been directly demonstrated yet for the apicomplexan centrosome
724 (Morlon-Guyot et al., 2017; Courjol and Gissot, 2018; Chen and Gubbels, 2019). At first sight,
725 contrasting insight comes from synchronized endodyogeny observed in *T. gondii* tachyzoites.
726 Upon completion of cell division, *T. gondii* daughters stay connected through a cytoplasmic actin

727 bridge maintained by Myosin I (Frenal et al., 2017b; Periz et al., 2017). If this bridge is intact, all
728 conjoined tachyzoites undergo endodyogeny in synchrony resulting in geometric expansion
729 numbers. However, the cell division cycles of parasites sharing the same vacuole become
730 uncoordinated if the bridge is disrupted. Strengthening this conclusion is the observation that 4-
731 5% of tachyzoites by chance form multiple (3-4) daughters per division round: the timing of
732 daughter budding is still synchronized with the other parasites in the vacuole despite the fact that
733 these tachyzoites have undergone two rounds of S/M phase (Hu et al., 2004). For signaling
734 purposes, these paradoxical "multi-daughter endodyogenic" parasites are still in the
735 synchronized cycle of "S/M coupled to budding" state consistent with endodyogeny.
736 Accumulating insights from various mutants displaying increased incidences of "multi-daughter
737 endodyogenic" parasites (Dubey et al., 2017) suggests that such parasites fail to start budding
738 because they are missing membrane building blocks to assemble the daughter IMC, and then slip
739 into the next cell cycle while remaining in the "S/M coupled to budding" state.
740 When karyokinesis does not follow each S/M phase polyploid nuclei are formed. In *S.*
741 *neurona* endopolygeny, karyokinesis does not occur at all till the onset of budding, but in
742 Heamosporidioan sporogenesis, karyokinesis is more optional, which leads to a mix of nuclei
743 with various levels of ploidy. However, the mitotic cycle within each nucleoplasm appears to be
744 coordinated (Gerald et al., 2011; Roques et al., 2015), suggesting this level of control is not at the
745 centrosome level, but likely the chromatin or nucleoplasm level. The control and mechanism of
746 karyokinesis are not understood, which is also the case in well-studied model eukaryotes
747 dividing by closed mitosis such as *Aspergillus nidulans*, fission yeast, and baker's yeast. The
748 challenge in polyploid nuclei is to keep the multiple sets of chromosomes together so they can be
749 accurately partitioned into the daughters. The solution is that the chromosomes remain clustered
750 throughout the cell cycle by tethering the centromeres to the nuclear lamina. For instance, in *T.*
751 *gondii* the 13 centromeres and associated kinetochores remain clustered at the centrocone, a
752 nuclear envelope fold that houses the spindle microtubules during mitosis (Brooks et al., 2011;
753 Farrell and Gubbels, 2014). Similar observations have been made throughout the *Plasmodium*
754 life cycle using kinetochore markers (Pandey et al., 2019). Strayed chromosomes are rarely
755 observed but individual centromeres are seen during interphase in the *Plasmodium* schizogony in
756 the red blood cell. However, all centromeres cluster together again at the spindle pole before
757 entering mitosis (Hoeijmakers et al., 2012). Clearly, centromere clustering and sequestration at

758 the nuclear envelope through the kinetochores is an effective strategy to warrant that complete
759 sets of chromosomes are maintained in polyploid nuclei.
760 None of the above addresses why there are two different forms of budding; i.e. internal vs
761 external. We will try to address this by looking at the phylogeny. The first question is whether
762 either internal budding or external budding are an innovation or ancestral process. Since not
763 enough cell division details are known for Apicomplexa outside those groups included in Fig 1, a
764 firm answer is not possible. In favor of loss of internal budding is the generally more reduced
765 genome and streamlined biology found in the *Plasmodium* spp. and the piroplasms (e.g. host cell
766 invasion (Gubbels and Duraisingh, 2012)). Alternatively, in favor of innovation of internal
767 budding in the cyst-forming Coccidia is the putative advantage evidenced during *T. gondii*
768 endodyogeny. In this case, the mother parasite remains invasion- and egress-competent
769 throughout most of the replication cycle, hence increasing the resilience of the parasite in the
770 dynamic host system (i.e. immune attacks) to move between host cells (Gaji et al., 2011). In
771 contrast, during *S. neurona* endopolygeny the micronemes disappear halfway through the
772 division process, which depletes their invasion capacity (Vaishnava et al., 2005); hence, this
773 model does not hold true for the polyploid internal budding modes. Alternatively, it can be
774 argued that the maintenance of a cortical cytoskeleton in the mother makes the parasites more
775 resistant to mechanical stress, but it is not immediately obvious how this sets the tissue cyst-
776 forming Coccidia apart from parasites dividing by external budding. As all of the Coccidia have
777 oral transmission routes, each species exhibits asexual stages in gut epithelial cells; indeed, the
778 non-cyst forming Coccidia complete their whole cycle in the intestinal epithelium. This
779 revelation suggests that the differentiation of internal from external budding might be coupled to
780 the innovation of tissue cyst formation. The requirements for cyst formation comprise dispersion
781 throughout the host beyond the gut-epithelium and assembly of the cyst in neuronal and/or
782 muscular tissue, which do not have obvious links to division modes. Both the tissue cyst
783 inhabiting bradyzoite stages of *T. gondii* and *S. neurona* (pre-bradyzoite metrocytes as well)
784 undergo endodyogeny; only the acute stage of *S. neurona* divides by endopolygeny (Dubey et
785 al., 2001). In addition, although the acute stage of *S. neurona* dissolves the vacuolar
786 compartment and replicates in the host cell cytoplasm, bradyzoite multiplication and cyst
787 formation occur within a vacuole (Jakel et al., 2001). Cyst expansion has to occur gradually so as
788 not to compromise the cyst wall, which obviously is more compatible with endodyogeny than

789 endopolygeny. Notably, bradyzoite replication within *T. gondii* cysts is asynchronous and is
790 consistent with this model (Watts et al., 2015).
791 An outlier is *Eimeria callospermophili,* a rodent parasite that replicates by endopolygeny
792 rather than schizogony, and as far as known, does not form tissue cysts (Roberts et al., 1970;
793 Hammond, 1973). *E. callospermophili* undergoes several rounds of S-phase that are each
794 followed by karyokinesis to produce 4-10 nuclei per schizont while the mother's cytoskeleton is
795 maintained. In synchrony, two daughters per nucleus bud internally and the plasma membrane is
796 acquired when the daughter are about 1/3 developed, resulting in 8-20 merozoites. This suggests
797 internal budding was likely present before the advent of tissue cyst formation. However, the
798 phylogenetic position of this parasite is on the edge of the *Eimeria* spp. (Fig 1). To complicate
799 matters further, genome information has demonstrated that the *Eimeria* spp. and the *Isopora* spp.
800 branch within each other and that neither are monophyletic clades (Kvicerova and Hypsa, 2013).
801 Furthermore, the mechanism of cortical budding occurs across the Coccidia sexual cycle during
802 microgametocyte formation (Ferguson et al., 1974; Ferguson et al., 2008). Hence, parasites can
803 exhibit both cell division modes at different stages of their life-cycles – internal and external
804 budding. We also know that sporozoite formation in *T. gondii* occurs through an internal budding
805 mechanism in the absence of a maternal cytoskeleton (Ferguson et al., 1979b; Dubey et al.,
806 2017). Interestingly, the timing of plasma membrane association with the cytoskeleton is much
807 earlier in this situation compared to the other asexual stages occurring in presence of a maternal
808 cytoskeleton, which indicates the timing of events is flexible. Taken together, there appears to be
809 a continuum between the morphogenic features of the Coccidia, suggesting that there is a
810 significant level of plasticity in biology and division modes. Further insights may result from the
811 investigation of parasite species straddling the two division modes; for example, the *Goussia*
812 spp. bridging the cyst-forming and non-cyst forming Coccidia (Fig 1) (Barta et al., 2001). The
813 *Goussia* spp. are found in fish, reptiles and amphibians, which have not been extensively studied
814 at the cell biological level (Rosenthal et al., 2016). Overall, why the two different extant forms of
815 budding exist cannot be answered with satisfaction based on the factors we considered.
816 This leaves the question of what the mechanistic differences are between internal and
817 external budding. The key question here is how parasites transitioned between the general
818 strategies of external vs internal budding. A principal difference is rooted in the localization of
819 the centrosome. In cortical budding the centrosomes reorient to the plasma membrane, whereas

820 during internal budding they remain in the cytoplasm. A simple model suggests that the presence
821 of the mother's cytoskeleton physically prevents access of the centrosome to the plasma
822 membrane. Yet, it is unlikely such a simplistic model fully describes this complicated process. A
823 structure anchoring the centrosome to the cortical cytoskeleton has been described for *T. gondii*
824 endodyogeny; a striated fiber assemblin (SFA), extending from the centrosome to the conoid
825 (Francia et al., 2012). SFA fibers are typically found in the flagellar assembly of algae, where
826 they contribute to orientation of the basal body rootlet system relative to other subcellular
827 structures (Francia et al., 2015). During *Eimeria necatrix* schizogony, a dense structure anchors
828 the centrosome to the plasma membrane. This structure migrates basally along with the cortical
829 microtubules during the progression of daughter bud assembly (Dubremetz, 1975), and might be
830 related to the SFA fiber. Such a structure has not been described for *Plasmodium* schizogony in
831 the red blood cell, although the SFA genes are conserved in *Plasmodium* spp. (Lechtreck, 2003) .
832 Thus, SFA-like structures anchoring the centrosome to the plasma membrane have been
833 observed in *Eimeria* schizogony (Dubremetz, 1971) and even in *Theileria equi* sporozoite
834 schizogony (Moltmann et al., 1983) and appear to be a differentiating factor between internal and
835 external budding. Further study of SFA genes across the Apicomplexa may reveal the nature of
836 how nuclei are anchored in the buds across the different division modes.
837 Several more principle difference between internal budding relative to cortical budding exist.
838 For example, the mother and daughter cytoskeletons must be differentially stabilized upon
839 completion of budding. What are the putative mechanisms? It has been shown that a timely
840 regulated proteolysis which removes the C-terminus of the major network component, IMC1,
841 coinciding with conversion of the network from a detergent-labile to a detergent-resistant state
842 late in *T. gondii* daughter cell development (Mann et al., 2002). On the other hand, ubiquitination
843 of the mother's cytoskeleton marks it for destruction (Silmon de Monerri et al., 2015; Dhara and
844 Sinai, 2016). Although the former informs about maturation and the latter about destabilization,
845 neither informs directly on the basis of differential stability. In parallel, some of the maternal
846 building blocks (e.g. IMC proteins, glideosome) are recycled in the final growth spurt of the
847 daughters (Ouologuem and Roos, 2014; Periz et al., 2019). An additional mechanism is provided
848 by differential components present on either mother (e.g. MSC1b (Lorestani et al., 2012),
849 GAP45 (Gaskins et al., 2004), or IMC7, 12, 14, 17, 18 and 20 (Anderson-White et al., 2011;
850 Chen et al., 2015a)) or daughter parasite (e.g. IMC16, 29 (Chen et al., 2015a; Chen et al., 2016)),

851 or swapping places from mother to daughter (e.g. SPM3, (Samad et al., 2015)). Such differential
852 composition of mother and daughters may be factors in differential stability, but to date no single
853 factor provides a satisfactory explanation.
854 Another potential problem posed by the mother's cytoskeleton during internal budding
855 occurs in the growth phase, where it restricts access to nutrients and complicates the ability to
856 expel waste. This is most relevant for the expanding cell during endopolygeny with large
857 cytoplasmic mass. Although both the apical and basal extremes of the cytoskeleton have
858 openings toward the plasma membrane, they are relatively small and it is not clear whether they
859 are sufficient for the level of exchange needed. However, it is not clear whether the sutures
860 between the alveoli are permeable for diffusion of small molecules, which would void this
861 argument. Either way, a set of apical annuli largely composed of AAP proteins residing in the
862 IMC sutures were recently suggested to function as pores across the IMC (Engelberg et al., 2019;
863 Lentini et al., 2019). In support of this hypothesis is the narrow conservation of AAP protein
864 orthologs only in the Sarcocystidae, indicating their function is most likely in support of internal
865 budding. However, disruption of apical annuli structure resulted in a minor fitness loss of *T.*
866 *gondii* tachyzoites, which might be because endodyogeny poses rather limited demands on
867 exchange, especially compared to endopolygenic replication modes where the mother
868 cytoskeleton could pose a much larger barrier. An alternative role for the apical annuli is as a
869 gateway for a burst in dense granule secretion following completion of invasion (Carruthers and
870 Sibley, 1997): electron microscopy studies place dense granule release at this moment in an
871 apical location consistent with the position of the annuli (Dubremetz et al., 1993). Additional
872 studies on the role of the annuli during endopolygeny are needed to firmly differentiate between
873 these two potential roles.
874 In conclusion, we define two principally different asexual cell division modes, external and
875 internal budding, which can both produce as few as two daughters per division round, but in
876 most situations produce many more daughters per division round. The bipartite centrosome
877 model and the identification of several regulators of cell cycle progression and checkpoints in
878 recent years provide a framework to explain these division modes, however the evolutionary
879 history and cell biological features defining, organizing and executing the various division
880 modes are much less clear. Expanding genetic and cell biological toolboxes for parasites
881 representing the various division modes provide exciting future avenues toward resolving the

882 exotic apicomplexan cell division modes and shedding light on the evolutionary pressures that
883 select for diversification and choices for different division modes at different developmental
884 stages.
885

886 **5 Conflict of Interest Statement**

887 The authors declare that the research was conducted in the absence of any commercial or
888 financial relationships that could be construed as a potential conflict of interest.
889

890 **6 Author Contributions Statement**

891 MG, HW, DH and MD conceived the experiments, HW performed the *C. suis* experiments, SD
892 and DH performed the *S. neurona* experiments, MG, CK, AP, BE, and CB performed the
893 *Babesia* experiments, KE and MG performed SIM microscopy, BE and IC performed electron
894 microscopy, MG wrote the manuscript and all authors edited the manuscript.
895

896 **7 Funding**

897 This study was supported by National Science Foundation (NSF) Major Research
898 Instrumentation grant 1626072, National Institute of Health grants AI110690 (MJG), AI110638
899 (MJG), AI128136 (MJG), AI144856 (MJG), and AI128480 (MTD), an American Heart
900 Association pre-doctoral fellowship19PRE34380106 (CDK), a Profillinien start-up grant of the
901 University of Veterinary Medicine Vienna PP16110262 (HLW), an Australian NHMRC CJ
902 Martin fellowship (BE), a post-doctoral fellowship grant 17POST33670577 (KE), a Knights
903 Templar Eye Foundation Career Starter Award (KE), and USDA NIFA grant 2009-65109-05918
904 (DKH). The funders had no role in study design, data collection and analysis, decision to
905 publish, or preparation of the manuscript.
906

907 **8 Acknowledgements**

908 We thank Bret Judson and the Boston College Imaging Core as well as Stephan Handschuh and
909 the Imaging Core of the University of Veterinary Medicine Vienna for infrastructure and
910 support, Drs. Naomi Morrissette, Jaime Tarigo, and Jeff Dvorin for discussion, and Drs. David
911 Allred, Kirk Deitsch and Laura Kirkman for sharing reagents.
912

913 **9 References**
914

915 Al-Khattaf, F.S., Tremp, A.Z., and Dessens, J.T. (2015). Plasmodium alveolins possess distinct
916 but structurally and functionally related multi-repeat domains. *Parasitol Res* 114**,** 631-
917 639.
918 Alexandrov, A., Vignali, M., Lacount, D.J., Quartley, E., De Vries, C., De Rosa, D., Babulski, J.,
919 Mitchell, S.F., Schoenfeld, L.W., Fields, S., Hol, W.G., Dumont, M.E., Phizicky, E.M.,
920 and Grayhack, E.J. (2004). A facile method for high-throughput co-expression of protein
921 pairs. *Mol Cell Proteomics* 3**,** 934-938.
922 Alvarez, C.A., and Suvorova, E.S. (2017). Checkpoints of apicomplexan cell division identified
923 in Toxoplasma gondii. *PLoS Pathog* 13**,** e1006483.
924 Anderson-White, B.R., Beck, J.R., Chen, C.T., Meissner, M., Bradley, P.J., and Gubbels, M.J.
925 (2012). Cytoskeleton assembly in Toxoplasma gondii cell division. *Int. Rev. Cell Mol.*
926 *Biol.* 298**,** 1-31.
927 Anderson-White, B.R., Ivey, F.D., Cheng, K., Szatanek, T., Lorestani, A., Beckers, C.J.,
928 Ferguson, D.J., Sahoo, N., and Gubbels, M.J. (2011). A family of intermediate filament-
929 like proteins is sequentially assembled into the cytoskeleton of Toxoplasma gondii. *Cell*
930 *Microbiol* 13**,** 18-31.
931 Angrisano, F., Tan, Y.H., Sturm, A., Mcfadden, G.I., and Baum, J. (2012). Malaria parasite
932 colonisation of the mosquito midgut--placing the Plasmodium ookinete centre stage. *Int J*
933 *Parasitol* 42**,** 519-527.
934 Araki, T., Kawai, S., Kakuta, S., Kobayashi, H., Umeki, Y., Saito-Nakano, Y., Sasaki, T.,
935 Nagamune, K., Yasutomi, Y., Nozaki, T., Franke-Fayard, B., Khan, S.M., Hisaeda, H.,
936 and Annoura, T. (2019). Three-dimensional electron microscopy analysis reveals
937 endopolygeny-like nuclear architecture segregation in Plasmodium oocyst development.
938 *Parasitol Int* 76**,** 102034.
939 Arnot, D.E., Ronander, E., and Bengtsson, D.C. (2011). The progression of the intra-erythrocytic
940 cell cycle of Plasmodium falciparum and the role of the centriolar plaques in
941 asynchronous mitotic division during schizogony. *Int J Parasitol* 41**,** 71-80.
942 Barta, J.R., Martin, D.S., Carreno, R.A., Siddall, M.E., Profous-Juchelkat, H., Hozza, M.,
943 Powles, M.A., and Sundermann, C. (2001). Molecular phylogeny of the other tissue
944 coccidia: Lankesterella and Caryospora. *J Parasitol* 87**,** 121-127.
945 Bennink, S., Kiesow, M.J., and Pradel, G. (2016). The development of malaria parasites in the
946 mosquito midgut. *Cell Microbiol* 18**,** 905-918.
947 Berry, L., Chen, C.T., Francia, M.E., Guerin, A., Graindorge, A., Saliou, J.M., Grandmougin,
948 M., Wein, S., Bechara, C., Morlon-Guyot, J., Bordat, Y., Gubbels, M.J., Lebrun, M.,
949 Dubremetz, J.F., and Daher, W. (2018). Toxoplasma gondii chromosomal passenger
950 complex is essential for the organization of a functional mitotic spindle: a prerequisite for
951 productive endodyogeny. *Cell Mol Life Sci* 75**,** 4417-4443.
952 Berry, L., Chen, C.T., Reininger, L., Carvalho, T.G., El Hajj, H., Morlon-Guyot, J., Bordat, Y.,
953 Lebrun, M., Gubbels, M.J., Doerig, C., and Daher, W. (2016). The conserved
954 apicomplexan Aurora kinase TgArk3 is involved in endodyogeny, duplication rate and
955 parasite virulence. *Cell Microbiol* 18**,** 1106-1120.
956 Bock, R., Jackson, L., De Vos, A., and Jorgensen, W. (2004). Babesiosis of cattle. *Parasitology*
957 129 Suppl**,** S247-269.

958 Bornens, M., and Gonczy, P. (2014). Centrosomes back in the limelight. *Philos Trans R Soc*
959 *Lond B Biol Sci* 369.
960 Brooks, C.F., Francia, M.E., Gissot, M., Croken, M.M., Kim, K., and Striepen, B. (2011).
961 Toxoplasma gondii sequesters centromeres to a specific nuclear region throughout the
962 cell cycle. *Proc Natl Acad Sci U S A* 108**,** 3767-3772.
963 Brown, K.M., Suvorova, E., Farrell, A., Wiley, B.B., Marth, G., Gaffney, P.M., Gubbels, M.-J.,
964 White, M., and J., B.I. (2014). Forward Genetic Screening Identifies a Small Molecule
965 that Blocks Toxoplasma gondii Growth By Inhibiting Both Host- and Parasite-Encoded
966 Kinases. *PLoS Pathog* 10**,** e1004180.
967 Canning, E.U., and Sinden, R.E. (1973). The organization of the ookinete and observations on
968 nuclear division in oocysts of Plasmodium berghei. *Parasitology* 67**,** 29-40.
969 Carruthers, V.B., and Sibley, L.D. (1997). Sequential protein secretion from three distinct
970 organelles of Toxoplasma gondii accompanies invasion of human fibroblasts. *Eur J Cell*
971 *Biol* 73**,** 114-123.
972 Carter, V., Nacer, A.M., Underhill, A., Sinden, R.E., and Hurd, H. (2007). Minimum
973 requirements for ookinete to oocyst transformation in Plasmodium. *Int J Parasitol* 37**,**
974 1221-1232.
975 Carvalho, T.G., Doerig, C., and Reininger, L. (2013). Nima- and Aurora-related kinases of
976 malaria parasites. *Biochim Biophys Acta* 1834**,** 1336-1345.
977 Chakraborty, S., Roy, S., Mistry, H.U., Murthy, S., George, N., Bhandari, V., and Sharma, P.
978 (2017). Potential Sabotage of Host Cell Physiology by Apicomplexan Parasites for Their
979 Survival Benefits. *Front Immunol* 8**,** 1261.
980 Chen, A.L., Kim, E.W., Toh, J.Y., Vashisht, A.A., Rashoff, A.Q., Van, C., Huang, A.S., Moon,
981 A.S., Bell, H.N., Bentolila, L.A., Wohlschlegel, J.A., and Bradley, P.J. (2015a). Novel
982 components of the Toxoplasma inner membrane complex revealed by BioID. *MBio* 6**,**
983 e02357-02314.
984 Chen, A.L., Moon, A.S., Bell, H.N., Huang, A.S., Vashisht, A.A., Toh, J.Y., Lin, A.H.,
985 Nadipuram, S.M., Kim, E.W., Choi, C.P., Wohlschlegel, J.A., and Bradley, P.J. (2016).
986 Novel insights into the composition and function of the Toxoplasma IMC sutures. *Cell*
987 *Microbiol*.
988 Chen, C.T., and Gubbels, M.-J. (2019). TgCep250 is dynamically processed through the division
989 cycle and essential for structural integrity of the Toxoplasma centrosome. *Mol Biol Cell*
990 30**,** 1160-1169.
991 Chen, C.T., and Gubbels, M.J. (2013). The Toxoplasma gondii centrosome is the platform for
992 internal daughter budding as revealed by a Nek1 kinase mutant. *J Cell Sci* 126**,** 3344-
993 3355.
994 Chen, C.T., Kelly, M., Leon, J., Nwagbara, B., Ebbert, P., Ferguson, D.J., Lowery, L.A.,
995 Morrissette, N., and Gubbels, M.J. (2015b). Compartmentalized Toxoplasma EB1
996 bundles spindle microtubules to secure accurate chromosome segregation. *Mol Biol Cell*
997 26**,** 4562-4576.
998 Conrad, P.A., Denham, D., and Brown, C.G. (1986). Intraerythrocytic multiplication of Theileria
999 parva in vitro: an ultrastructural study. *Int J Parasitol* 16**,** 223-229.
1000 Conrad, P.A., Kelly, B.G., and Brown, C.G. (1985). Intraerythrocytic schizogony of Theileria
1001 annulata. *Parasitology* 91 (Pt 1)**,** 67-82.
1002 Conrad, P.A., Kjemtrup, A.M., Carreno, R.A., Thomford, J., Wainwright, K., Eberhard, M.,
1003 Quick, R., Telford, S.R., 3rd, and Herwaldt, B.L. (2006). Description of Babesia duncani

1004 n.sp. (Apicomplexa: Babesiidae) from humans and its differentiation from other
1005 piroplasms. *Int J Parasitol* 36**,** 779-789.
1006 Courjol, F., and Gissot, M. (2018). A coiled-coil protein is required for coordination of
1007 karyokinesis and cytokinesis in Toxoplasma gondii. *Cell Microbiol* 20**,** e12832.
1008 De Leon, J.C., Scheumann, N., Beatty, W., Beck, J.R., Tran, J.Q., Yau, C., Bradley, P.J., Gull,
1009 K., Wickstead, B., and Morrissette, N.S. (2013). A SAS-6-like protein suggests that the
1010 Toxoplasma conoid complex evolved from flagellar components. *Eukaryot Cell* 12**,**
1011 1009-1019.
1012 Dhara, A., and Sinai, A.P. (2016). A Cell Cycle-Regulated Toxoplasma Deubiquitinase,
1013 TgOTUD3A, Targets Polyubiquitins with Specific Lysine Linkages. *mSphere* 1.
1014 Dubey, J.P., Lindsay, D.S., Fritz, D., and Speer, C.A. (2001). Structure of Sarcocystis neurona
1015 sarcocysts. *J Parasitol* 87**,** 1323-1327.
1016 Dubey, R., Harrison, B., Dangoudoubiyam, S., Bandini, G., Cheng, K., Kosber, A., Agop-
1017 Nersesian, C., Howe, D.K., Samuelson, J., Ferguson, D.J.P., and Gubbels, M.J. (2017).
1018 Differential Roles for Inner Membrane Complex Proteins across Toxoplasma gondii and
1019 Sarcocystis neurona Development. *mSphere* 2.
1020 Dubey, R., Staker, B.L., Foe, I.T., Bogyo, M., Myler, P.J., Ngo, H.M., and Gubbels, M.J. (2016).
1021 Membrane skeletal association and post-translational allosteric regulation of Toxoplasma
1022 gondii GAPDH1. *Mol Microbiol*.
1023 Dubremetz, J.F. (1971). L'ultrastructure du centriole et du centrocone chez la coccidie eimeria
1024 necatrix. Étude au cours de la schizogonie. *J Microsc.* 23**,** 453–458.
1025 Dubremetz, J.F. (1973). [Ultrastructural study of schizogonic mitosis in the coccidian, Eimeria
1026 necatrix (Johnson 1930)]. *J Ultrastruct Res* 42**,** 354-376.
1027 Dubremetz, J.F. (1975). [Genesis of merozoites in the coccidia, Eimeria necatrix. Ultrastructural
1028 study]. *J Protozool* 22**,** 71-84.
1029 Dubremetz, J.F., Achbarou, A., Bermudes, D., and Joiner, K.A. (1993). Kinetics and pattern of
1030 organelle exocytosis during Toxoplasma gondii/host-cell interaction. *Parasitol Res* 79**,**
1031 402-408.
1032 Dubremetz, J.F., and Elsner, Y.Y. (1979). Ultrastructural study of schizogony of Eimeria bovis
1033 in cell cultures. *J Protozool* 26**,** 367-376.
1034 Engelberg, K., Chen, C.-T., Bechtel, T., Sánchez Guzmán, V., Drozda, A.A., Chavan, S.,
1035 Weerapana, E., and Gubbels, M.-J. (2019). The apical annuli of Toxoplasma gondii are
1036 composed of coiled-coil and signaling proteins embedded in the IMC sutures. *BioRXiv*
1037 doi.org/10.1101/711432
1038 Farrell, M., and Gubbels, M.J. (2014). The Toxoplasma gondii kinetochore is required for
1039 centrosome association with the centrocone (spindle pole). *Cellular Microbiology* 16**,** 78-
1040 94.
1041 Fawcett, D.W., Conrad, P.A., Grootenhuis, J.G., and Morzaria, S.P. (1987). Ultrastructure of the
1042 intra-erythrocytic stage of Theileria species from cattle and waterbuck. *Tissue Cell* 19**,**
1043 643-655.
1044 Ferguson, D.J., Birch-Andersen, A., Hutchison, W.M., and Siim, J.C. (1980). Ultrastructural
1045 observations on microgametogenesis and the structure of the microgamete of Isospora
1046 felis. *Acta Pathol Microbiol Scand [B]* 88**,** 151-159.
1047 Ferguson, D.J., Birch-Andersen, A., Siim, J.C., and Hutchison, W.M. (1979a). Ultrastructural
1048 studies on the sporulation of oocysts of Toxoplasma gondii. I. Development of the zygote

1049 and formation of the sporoblasts. *Acta pathologica et microbiologica Scandinavica.*
1050 *Section B, Microbiology* 87B**,** 171-181.
1051 Ferguson, D.J., Birch-Andersen, A., Siim, J.C., and Hutchison, W.M. (1979b). Ultrastructural
1052 studies on the sporulation of oocysts of Toxoplasma gondii. III. Formation of the
1053 sporozoites within the sporocysts. *Acta pathologica et microbiologica Scandinavica.*
1054 *Section B, Microbiology* 87**,** 253-260.
1055 Ferguson, D.J., Hutchison, W.M., Dunachie, J.F., and Siim, J.C. (1974). Ultrastructural study of
1056 early stages of asexual multiplication and microgametogony of Toxoplasma gondii in the
1057 small intestine of the cat. *Acta Pathol Microbiol Scand [B] Microbiol Immunol* 82**,** 167-
1058 181.
1059 Ferguson, D.J., Sahoo, N., Pinches, R.A., Bumstead, J.M., Tomley, F.M., and Gubbels, M.J.
1060 (2008). MORN1 has a conserved role in asexual and sexual development across the
1061 Apicomplexa. *Eukaryot Cell* 7**,** 698-711.
1062 Francia, M.E., Dubremetz, J.F., and Morrissette, N.S. (2015). Basal body structure and
1063 composition in the apicomplexans Toxoplasma and Plasmodium. *Cilia* 5**,** 3.
1064 Francia, M.E., Jordan, C.N., Patel, J.D., Sheiner, L., Demerly, J.L., Fellows, J.D., De Leon, J.C.,
1065 Morrissette, N.S., Dubremetz, J.F., and Striepen, B. (2012). Cell division in
1066 Apicomplexan parasites is organized by a homolog of the striated rootlet fiber of algal
1067 flagella. *PLoS biology* 10**,** e1001444.
1068 Francia, M.E., and Striepen, B. (2014). Cell division in apicomplexan parasites. *Nature reviews.*
1069 *Microbiology* 12**,** 125-136.
1070 Frenal, K., Dubremetz, J.F., Lebrun, M., and Soldati-Favre, D. (2017a). Gliding motility powers
1071 invasion and egress in Apicomplexa. *Nat Rev Microbiol* 15**,** 645-660.
1072 Frenal, K., Jacot, D., Hammoudi, P.M., Graindorge, A., Maco, B., and Soldati-Favre, D. (2017b).
1073 Myosin-dependent cell-cell communication controls synchronicity of division in acute
1074 and chronic stages of Toxoplasma gondii. *Nat Commun* 8**,** 15710.
1075 Frenal, K., Marq, J.B., Jacot, D., Polonais, V., and Soldati-Favre, D. (2014). Plasticity between
1076 MyoC- and MyoA-glideosomes: an example of functional compensation in Toxoplasma
1077 gondii invasion. *PLoS Pathog* 10**,** e1004504.
1078 Friedhoff, K.T., and Scholtyseck, E. (1977). Fine structural identification of erythrocytic stages
1079 of Babesia bigemina, Babesia divergens and Balesia ovis. *Protistologica* 13**,** 195-204.
1080 Fung, C., Beck, J.R., Robertson, S.D., Gubbels, M.J., and Bradley, P.J. (2012). Toxoplasma ISP4
1081 is a central IMC sub-compartment protein whose localization depends on palmitoylation
1082 but not myristoylation. *Mol Biochem Parasitol* 184**,** 99-108.
1083 Gaji, R.Y., Behnke, M.S., Lehmann, M.M., White, M.W., and Carruthers, V.B. (2011). Cell
1084 cycle-dependent, intercellular transmission of Toxoplasma gondii is accompanied by
1085 marked changes in parasite gene expression. *Mol Microbiol* 79**,** 192-204.
1086 Ganter, M., Goldberg, J.M., Dvorin, J.D., Paulo, J.A., King, J.G., Tripathi, A.K., Paul, A.S.,
1087 Yang, J., Coppens, I., Jiang, R.H., Elsworth, B., Baker, D.A., Dinglasan, R.R., Gygi, S.P.,
1088 and Duraisingh, M.T. (2017). Plasmodium falciparum CRK4 directs continuous rounds
1089 of DNA replication during schizogony. *Nat Microbiol* 2**,** 17017.
1090 Gardiner, C.H., Fayer, R., and Dubey, J.P. (1998). *An Atlas of Protozoan Parasites in Animal*
1091 *Tissues.* Armed Forces Institute of Pathology.
1092 Gaskins, E., Gilk, S., Devore, N., Mann, T., Ward, G., and Beckers, C. (2004). Identification of
1093 the membrane receptor of a class XIV myosin in Toxoplasma gondii. *J Cell Biol* 165**,**
1094 383-393.

1095 Gerald, N., Mahajan, B., and Kumar, S. (2011). Mitosis in the human malaria parasite
1096 Plasmodium falciparum. *Eukaryot Cell* 10**,** 474-482.
1097 Goldman, M., Carver, R.K., and Sulzer, A.J. (1958). Reproduction of Toxoplasma gondii by
1098 internal budding. *J Parasitol* 44**,** 161-171.
1099 Goodenough, U., Roth, R., Kariyawasam, T., He, A., and Lee, J.H. (2018). Epiplasts: Membrane
1100 Skeletons and Epiplastin Proteins in Euglenids, Glaucophytes, Cryptophytes, Ciliates,
1101 Dinoflagellates, and Apicomplexans. *MBio* 9.
1102 Gould, S.B., Tham, W.H., Cowman, A.F., Mcfadden, G.I., and Waller, R.F. (2008). Alveolins, a
1103 new family of cortical proteins that define the protist infrakingdom Alveolata. *Mol Biol*
1104 *Evol* 25**,** 1219-1230.
1105 Gruring, C., Heiber, A., Kruse, F., Ungefehr, J., Gilberger, T.W., and Spielmann, T. (2011).
1106 Development and host cell modifications of Plasmodium falciparum blood stages in four
1107 dimensions. *Nat Commun* 2**,** 165.
1108 Gubbels, M.J., and Duraisingh, M.T. (2012). Evolution of apicomplexan secretory organelles. *Int*
1109 *J Parasitol* 42**,** 1071-1081.
1110 Gubbels, M.J., Vaishnava, S., Boot, N., Dubremetz, J.F., and Striepen, B. (2006). A MORN-
1111 repeat protein is a dynamic component of the Toxoplasma gondii cell division apparatus.
1112 *J Cell Sci* 119**,** 2236-2245.
1113 Gubbels, M.J., Wieffer, M., and Striepen, B. (2004). Fluorescent protein tagging in Toxoplasma
1114 gondii: identification of a novel inner membrane complex component conserved among
1115 Apicomplexa. *Mol Biochem Parasitol* 137**,** 99-110.
1116 Hammond, D.M. (1973). *The Coccidia: Eimeria, Isospora, Toxoplasma, and related genera.*
1117 University Park Press.
1118 Heaslip, A.T., Dzierszinski, F., Stein, B., and Hu, K. (2010). TgMORN1 Is a Key Organizer for
1119 the Basal Complex of Toxoplasma gondii. *PLoS Pathog* 6**,** e1000754.
1120 Hepler, P.K., Huff, C.G., and Sprinz, H. (1966). The fine structure of the exoerythrocytic stages
1121 of Plasmodium fallax. *J Cell Biol* 30**,** 333-358.
1122 Hoeijmakers, W.A., Flueck, C., Francoijs, K.J., Smits, A.H., Wetzel, J., Volz, J.C., Cowman,
1123 A.F., Voss, T., Stunnenberg, H.G., and Bartfai, R. (2012). Plasmodium falciparum
1124 centromeres display a unique epigenetic makeup and cluster prior to and during
1125 schizogony. *Cell Microbiol* 14**,** 1391-1401.
1126 Howe, D.K., Yeargan, M., Simpson, L., and Dangoudoubiyam, S. (2018). Molecular Genetic
1127 Manipulation of Sarcocystis neurona. *Curr Protoc Microbiol* 48**,** 20D 22 21-20D 22 14.
1128 Howells, R.E., and Davies, E.E. (1971a). Nuclear division in the oocyst of Plasmodium berghei.
1129 *Ann Trop Med Parasitol* 65**,** 451-459.
1130 Howells, R.E., and Davies, E.E. (1971b). Post-meiotic nuclear divisions in the oocyst of
1131 Plasmodium berghei. *Trans R Soc Trop Med Hyg* 65**,** 421.
1132 Hu, K. (2008). Organizational changes of the daughter basal complex during the parasite
1133 replication of Toxoplasma gondii. *PLoS Pathog* 4**,** e10.
1134 Hu, K., Johnson, J., Florens, L., Fraunholz, M., Suravajjala, S., Dilullo, C., Yates, J., Roos, D.S.,
1135 and Murray, J.M. (2006). Cytoskeletal components of an invasion machine--the apical
1136 complex of Toxoplasma gondii. *PLoS Pathog* 2**,** e13.
1137 Hu, K., Roos, D.S., Angel, S.O., and Murray, J.M. (2004). Variability and heritability of cell
1138 division pathways in Toxoplasma gondii. *J Cell Sci* 117**,** 5697-5705.
1139 Jakel, T., Wallstein, E., Muncheberg, F., Archer-Baumann, C., Weingarten, B., Kliemt, D., and
1140 Mackenstedt, U. (2001). Binding of a monoclonal antibody to sporozoites of Sarcocystis

1141 singaporensis enhances escape from the parasitophorous vacuole, which is necessary for
1142 intracellular development. *Infect Immun* 69**,** 6475-6482.
1143 Jalovecka, M., Hajdusek, O., Sojka, D., Kopacek, P., and Malandrin, L. (2018). The Complexity
1144 of Piroplasms Life Cycles. *Front Cell Infect Microbiol* 8**,** 248.
1145 Jayabalasingham, B., Bano, N., and Coppens, I. (2010). Metamorphosis of the malaria parasite in
1146 the liver is associated with organelle clearance. *Cell Res* 20**,** 1043-1059.
1147 Jerka-Dziadosz, M., and Frankel, J. (1995). The effects of lithium chloride on pattern formation
1148 in Tetrahymena thermophila. *Dev Biol* 171**,** 497-506.
1149 Jerka-Dziadosz, M., Jenkins, L.M., Nelsen, E.M., Williams, N.E., Jaeckel-Williams, R., and
1150 Frankel, J. (1995). Cellular polarity in ciliates: persistence of global polarity in a
1151 disorganized mutant of Tetrahymena thermophila that disrupts cytoskeletal organization.
1152 *Dev Biol* 169**,** 644-661.
1153 Joyner, L.P., and Long, P.L. (1974). The specific characters of the Eimeria, with special
1154 reference to the coccidia of the fowl. *Avian Pathol* 3**,** 145-157.
1155 Kono, M., Heincke, D., Wilcke, L., Wong, T., Bruns, C., Herrmann, S., Spielmann, T., and
1156 Gilberger, T.W. (2016). Pellicle formation in the malaria parasite. *J Cell Sci*.
1157 Kono, M., Herrmann, S., Loughran, N.B., Cabrera, A., Engelberg, K., Lehmann, C., Sinha, D.,
1158 Prinz, B., Ruch, U., Heussler, V., Spielmann, T., Parkinson, J., and Gilberger, T.W.
1159 (2012). Evolution and Architecture of the Inner Membrane Complex in Asexual and
1160 Sexual Stages of the Malaria Parasite. *Molecular biology and evolution* 29**,** 2113-2132.
1161 Kvicerova, J., and Hypsa, V. (2013). Host-parasite incongruences in rodent Eimeria suggest
1162 significant role of adaptation rather than cophylogeny in maintenance of host specificity.
1163 *PLoS One* 8**,** e63601.
1164 Le Roch, K., Sestier, C., Dorin, D., Waters, N., Kappes, B., Chakrabarti, D., Meijer, L., and
1165 Doerig, C. (2000). Activation of a Plasmodium falciparum cdc2-related kinase by
1166 heterologous p25 and cyclin H. Functional characterization of a P. falciparum cyclin
1167 homologue. *J Biol Chem* 275**,** 8952-8958.
1168 Leander, B.S., and Keeling, P.J. (2003). Morphostasis in alveolate evolution. *trends in Ecology*
1169 *and Evolution* 18**,** 395-402.
1170 Lechtreck, K.F. (2003). Striated fiber assemblin in apicomplexan parasites. *Mol Biochem*
1171 *Parasitol* 128**,** 95-99.
1172 Lentini, G., Dubois, D.J., Maco, B., Soldati-Favre, D., and Frenal, K. (2019). The roles of
1173 Centrin 2 and Dynein Light Chain 8a in apical secretory organelles discharge of
1174 Toxoplasma gondii. *Traffic*.
1175 Lindsay, D.S., Stuart, B.P., Wheat, B.E., and Ernst, J.V. (1980). Endogenous development of the
1176 swine coccidium, Isospora suis Biester 1934. *J Parasitol* 66**,** 771-779.
1177 Lorestani, A., Ivey, F.D., Thirugnanam, S., Busby, M.A., Marth, G.T., Cheeseman, I.M., and
1178 Gubbels, M.J. (2012). Targeted proteomic dissection of Toxoplasma cytoskeleton sub-
1179 compartments using MORN1. *Cytoskeleton* 69**,** 1069-1085.
1180 Lorestani, A., Sheiner, L., Yang, K., Robertson, S.D., Sahoo, N., Brooks, C.F., Ferguson, D.J.,
1181 Striepen, B., and Gubbels, M.J. (2010). A Toxoplasma MORN1 Null Mutant Undergoes
1182 Repeated Divisions but Is Defective in Basal Assembly, Apicoplast Division and
1183 Cytokinesis. *PLoS ONE* 5**,** e12302.
1184 Luder, C.G., Stanway, R.R., Chaussepied, M., Langsley, G., and Heussler, V.T. (2009).
1185 Intracellular survival of apicomplexan parasites and host cell modification. *Int J Parasitol*
1186 39**,** 163-173.

1187 Mahajan, B., Selvapandiyan, A., Gerald, N.J., Majam, V., Zheng, H., Wickramarachchi, T.,
1188 Tiwari, J., Fujioka, H., Moch, J.K., Kumar, N., Aravind, L., Nakhasi, H.L., and Kumar,
1189 S. (2008). Centrins, cell cycle regulation proteins in human malaria parasite Plasmodium
1190 falciparum. *J Biol Chem* 283**,** 31871-31883.
1191 Mann, T., Gaskins, E., and Beckers, C. (2002). Proteolytic Processing of TgIMC1 during
1192 Maturation of the Membrane Skeleton of Toxoplasma gondii. *J Biol Chem* 277**,** 41240-
1193 41246.
1194 Martorelli Di Genova, B., Wilson, S.K., Dubey, J.P., and Knoll, L.J. (2019). Intestinal delta-6-
1195 desaturase activity determines host range for Toxoplasma sexual reproduction. *PLoS Biol*
1196 17**,** e3000364.
1197 Matthews, H., Duffy, C.W., and Merrick, C.J. (2018). Checks and balances? DNA replication
1198 and the cell cycle in Plasmodium. *Parasit Vectors* 11**,** 216.
1199 Matuschka, F.R., and Heydorn, A.O. (1980). "Die Entwicklung von Isospora suis Biester und
1200 Murray 1934 (Sporozoa : Coccidia : Eimeriidae) im Schwein," in *Zoologische Beiträge,*
1201 ed. K. Herter. (Berlin: Duncker & Humblot), 405-476.
1202 Mecklenburg, K.L. (2007). Drosophila retinophilin contains MORN repeats and is conserved in
1203 humans. *Mol Genet Genomics* 277**,** 481-489.
1204 Mehlhorn, H., and Shein, E. (1984). The piroplasms: life cycle and sexual stages. *Adv Parasitol*
1205 23**,** 37-103.
1206 Merckx, A., Le Roch, K., Nivez, M.P., Dorin, D., Alano, P., Gutierrez, G.J., Nebreda, A.R.,
1207 Goldring, D., Whittle, C., Patterson, S., Chakrabarti, D., and Doerig, C. (2003).
1208 Identification and initial characterization of three novel cyclin-related proteins of the
1209 human malaria parasite Plasmodium falciparum. *J Biol Chem* 278**,** 39839-39850.
1210 Moltmann, U.G., Mehlhorn, H., and Friedhoff, K.T. (1982). Ultrastructural study of the
1211 development of Babesia ovis (Piroplasmia) in the ovary of the vector tick Rhipicephalus
1212 bursa. *J Protozool* 29**,** 30-38.
1213 Moltmann, U.G., Mehlhorn, H., Schein, E., Voigt, W.P., and Friedhoff, K.T. (1983).
1214 Ultrastructural study on the development of Babesia equi (Coccidia: Piroplasmia) in the
1215 salivary glands of its vector ticks. *J Protozool* 30**,** 218-225.
1216 Morlon-Guyot, J., Francia, M.E., Dubremetz, J.F., and Daher, W. (2017). Towards a molecular
1217 architecture of the centrosome in Toxoplasma gondii. *Cytoskeleton (Hoboken)* 74**,** 55-71.
1218 Morriswood, B., and Schmidt, K. (2015). A MORN Repeat Protein Facilitates Protein Entry into
1219 the Flagellar Pocket of Trypanosoma brucei. *Eukaryot Cell* 14**,** 1081-1093.
1220 Naumov, A., Kratzer, S., Ting, L.M., Kim, K., Suvorova, E.S., and White, M.W. (2017). The
1221 Toxoplasma Centrocone Houses Cell Cycle Regulatory Factors. *MBio* 8.
1222 Nishi, M., Hu, K., Murray, J.M., and Roos, D.S. (2008). Organellar dynamics during the cell
1223 cycle of Toxoplasma gondii. *J Cell Sci* 121**,** 1559-1568.
1224 Nishikawa, Y., Quittnat, F., Stedman, T.T., Voelker, D.R., Choi, J.Y., Zahn, M., Yang, M.,
1225 Pypaert, M., Joiner, K.A., and Coppens, I. (2005). Host cell lipids control cholesteryl
1226 ester synthesis and storage in intracellular Toxoplasma. *Cell Microbiol* 7**,** 849-867.
1227 Ouologuem, D.T., and Roos, D.S. (2014). Dynamics of the Toxoplasma gondii inner membrane
1228 complex. *J Cell Sci* 127**,** 3320-3330.
1229 Pandey, R., Zeeshan, M., Ferguson, D.J.P., Markus, R., Brady, D., Daniel, E., Stanway, R.R.,
1230 Holder, A.A., Guttery, D.S., and Tewari, R. (2019). Real-time dynamics of Plasmodium
1231 NDC80 as a marker for the kinetochore during atypical mitosis and meiosis. *bioRxiv*
1232 http://dx.doi.org/10.1101/767830.

1233 Paul, A.S., Moreira, C.K., Elsworth, B., Allred, D.R., and Duraisingh, M.T. (2016). Extensive
1234 Shared Chemosensitivity between Malaria and Babesiosis Blood-Stage Parasites.
1235 *Antimicrob Agents Chemother* 60**,** 5059-5063.
1236 Periz, J., Del Rosario, M., Mcstea, A., Gras, S., Loney, C., Wang, L., Martin-Fernandez, M.L.,
1237 and Meissner, M. (2019). A highly dynamic F-actin network regulates transport and
1238 recycling of micronemes in Toxoplasma gondii vacuoles. *Nat Commun* 10**,** 4183.
1239 Periz, J., Whitelaw, J., Harding, C., Gras, S., Del Rosario Minina, M.I., Latorre-Barragan, F.,
1240 Lemgruber, L., Reimer, M.A., Insall, R., Heaslip, A., and Meissner, M. (2017).
1241 Toxoplasma gondii F-actin forms an extensive filamentous network required for material
1242 exchange and parasite maturation. *Elife* 6.
1243 Potgieter, F.T., and Els, H.J. (1976). Light and electron microscopic observations on the
1244 development of small merozoites of Babesia bovis in Boophilus microplus larvae.
1245 *Onderstepoort J Vet Res* 43**,** 123-128.
1246 Potgieter, F.T., and Els, H.J. (1977). The fine structure of intra-erythrocytic stages of Babesia
1247 bigemina. *Onderstepoort J Vet Res* 44**,** 157-168.
1248 Reed, S.M., Furr, M., Howe, D.K., Johnson, A.L., Mackay, R.J., Morrow, J.K., Pusterla, N., and
1249 Witonsky, S. (2016). Equine Protozoal Myeloencephalitis: An Updated Consensus
1250 Statement with a Focus on Parasite Biology, Diagnosis, Treatment, and Prevention. *J Vet*
1251 *Intern Med* 30**,** 491-502.
1252 Reilly, H.B., Wang, H., Steuter, J.A., Marx, A.M., and Ferdig, M.T. (2007). Quantitative
1253 dissection of clone-specific growth rates in cultured malaria parasites. *Int J Parasitol* 37**,**
1254 1599-1607.
1255 Reininger, L., Wilkes, J.M., Bourgade, H., Miranda-Saavedra, D., and Doerig, C. (2011). An
1256 essential Aurora-related kinase transiently associates with spindle pole bodies during
1257 Plasmodium falciparum erythrocytic schizogony. *Mol Microbiol* 79**,** 205-221.
1258 Robbins, J.A., Absalon, S., Streva, V.A., and Dvorin, J.D. (2017). The Malaria Parasite Cyclin H
1259 Homolog PfCyc1 Is Required for Efficient Cytokinesis in Blood-Stage Plasmodium
1260 falciparum. *MBio* 8.
1261 Roberts, R., Lister, I., Schmitz, S., Walker, M., Veigel, C., Trinick, J., Buss, F., and Kendrick-
1262 Jones, J. (2004). Myosin VI: cellular functions and motor properties. *Philosophical*
1263 *transactions of the Royal Society of London. Series B, Biological sciences* 359**,** 1931-
1264 1944.
1265 Roberts, W.L., Hammond, D.M., Anderson, L.C., and Speer, C.A. (1970). Ultrastructural study
1266 of schizogony in Eimeria callospermophili. *J Protozool* 17**,** 584-592.
1267 Roques, M., Stanway, R.R., Rea, E.I., Markus, R., Brady, D., Holder, A.A., Guttery, D.S., and
1268 Tewari, R. (2019). Plasmodium centrin PbCEN-4 localizes to the putative MTOC and is
1269 dispensable for malaria parasite proliferation. *Biol Open* 8.
1270 Roques, M., Wall, R.J., Douglass, A.P., Ramaprasad, A., Ferguson, D.J., Kaindama, M.L.,
1271 Brusini, L., Joshi, N., Rchiad, Z., Brady, D., Guttery, D.S., Wheatley, S.P., Yamano, H.,
1272 Holder, A.A., Pain, A., Wickstead, B., and Tewari, R. (2015). Plasmodium P-Type
1273 Cyclin CYC3 Modulates Endomitotic Growth during Oocyst Development in
1274 Mosquitoes. *PLoS Pathog* 11**,** e1005273.
1275 Rosenthal, B.M., Dunams-Morel, D., Ostoros, G., and Molnar, K. (2016). Coccidian parasites of
1276 fish encompass profound phylogenetic diversity and gave rise to each of the major
1277 parasitic groups in terrestrial vertebrates. *Infect Genet Evol* 40**,** 219-227.

1278 Rudlaff, R.M., Kraemer, S., Streva, V.A., and Dvorin, J.D. (2019). An essential contractile ring
1279 protein controls cell division in Plasmodium falciparum. *Nat Commun* 10**,** 2181.
1280 Rudzinska, M.A. (1981). "Morphologic aspects of host-cell-parasite relationships in babesiosis,"
1281 in *Babesiosis,* eds. M. Ristic & J.P. Kreier. (New York, NY: Academic Press), 87–142.
1282 Samad, N., Hliscs, M., Katris, N.J., Mcfadden, G.I., and Waller, R.F. (2015). Microtubule
1283 associated protein SPM3 shows dynamic repositioning during cytokinesis and is required
1284 for nascent daughter formation. *13th International Congress on Toxoplasmosis &*
1285 *Toxoplasma gondii Biology, At Gettysburg College, in Gettysburg PA (USA)*
1286 http://hdl.handle.net/11343/194103**,** 190.
1287 Schein, E., Mehlhorn, H., and Voigt, W.P. (1979). Electron microscopical studies on the
1288 development of Babesia canis (Sporozoa) in the salivary glands of the vector tick
1289 Dermacentor reticulatus. *Acta Trop* 36**,** 229-241.
1290 Scholtyseck, E. (1979). *Fine Structure of Parasitic Protozoa.* Springer.
1291 Schrevel, J., Asfaux-Foucher, G., and Bafort, J.M. (1977). [Ultrastructural study of multiple
1292 mitoses during sporogony of Plasmodium b. berghei]. *J Ultrastruct Res* 59**,** 332-350.
1293 Sharma, P., and Chitnis, C.E. (2013). Key molecular events during host cell invasion by
1294 Apicomplexan pathogens. *Curr Opin Microbiol* 16**,** 432-437.
1295 Shaw, M.K., and Tilney, L.G. (1992). How individual cells develop from a syncytium:
1296 merogony in Theileria parva (Apicomplexa). *J Cell Sci* 101 (Pt 1)**,** 109-123.
1297 Sheffield, H.G., and Melton, M.L. (1968). The fine structure and reproduction of Toxoplasma
1298 gondii. *J Parasitol* 54**,** 209-226.
1299 Shetty, J., Klotz, K.L., Wolkowicz, M.J., Flickinger, C.J., and Herr, J.C. (2007). Radial spoke
1300 protein 44 (human meichroacidin) is an axonemal alloantigen of sperm and cilia. *Gene*
1301 396**,** 93-107.
1302 Shrestha, A., Abd-Elfattah, A., Freudenschuss, B., Hinney, B., Palmieri, N., Ruttkowski, B., and
1303 Joachim, A. (2015). Cystoisospora suis - A Model of Mammalian Cystoisosporosis.
1304 *Front Vet Sci* 2**,** 68.
1305 Sievers, F., Wilm, A., Dineen, D., Gibson, T.J., Karplus, K., Li, W., Lopez, R., Mcwilliam, H.,
1306 Remmert, M., Soding, J., Thompson, J.D., and Higgins, D.G. (2011). Fast, scalable
1307 generation of high-quality protein multiple sequence alignments using Clustal Omega.
1308 *Mol Syst Biol* 7**,** 539.
1309 Silmon De Monerri, N.C., Yakubu, R.R., Chen, A.L., Bradley, P.J., Nieves, E., Weiss, L.M., and
1310 Kim, K. (2015). The Ubiquitin Proteome of Toxoplasma gondii Reveals Roles for Protein
1311 Ubiquitination in Cell-Cycle Transitions. *Cell Host Microbe* 18**,** 621-633.
1312 Simonetti, A.B. (1996). The biology of malarial parasite in the mosquito--a review. *Mem Inst*
1313 *Oswaldo Cruz* 91**,** 519-541.
1314 Sinden, R.E. (1983). Sexual development of malarial parasites. *Adv Parasitol* 22**,** 153-216.
1315 Sinden, R.E., Canning, E.U., Bray, R.S., and Smalley, M.E. (1978). Gametocyte and gamete
1316 development in Plasmodium falciparum. *Proc R Soc Lond B Biol Sci* 201**,** 375-399.
1317 Sinden, R.E., and Strong, K. (1978). An ultrastructural study of the sporogonic development of
1318 Plasmodium falciparum in Anopheles gambiae. *Trans R Soc Trop Med Hyg* 72**,** 477-491.
1319 Spreng, B., Fleckenstein, H., Kubler, P., Di Biagio, C., Benz, M., Patra, P., Schwarz, U.S.,
1320 Cyrklaff, M., and Frischknecht, F. (2019). Microtubule number and length determine
1321 cellular shape and function in Plasmodium. *EMBO J* 38**,** e100984.

1322 Stanway, R.R., Mueller, N., Zobiak, B., Graewe, S., Froehlke, U., Zessin, P.J., Aepfelbacher, M.,
1323 and Heussler, V.T. (2011). Organelle segregation into Plasmodium liver stage
1324 merozoites. *Cell Microbiol* 13**,** 1768-1782.
1325 Stuart, B.P., Bedell, D.M., and Lindsay, D.S. (1982). Coccidiosis in swine: a search for
1326 extraintestinal stages of Isospora suis. *Vet Rec* 110**,** 82-83.
1327 Suarez, C.E., Alzan, H.F., Silva, M.G., Rathinasamy, V., Poole, W.A., and Cooke, B.M. (2019).
1328 Unravelling the cellular and molecular pathogenesis of bovine babesiosis: is the sky the
1329 limit? *Int J Parasitol* 49**,** 183-197.
1330 Sugi, T., Kawazu, S., Horimoto, T., and Kato, K. (2015). A single mutation in the gatekeeper
1331 residue in TgMAPKL-1 restores the inhibitory effect of a bumped kinase inhibitor on the
1332 cell cycle. *Int J Parasitol Drugs Drug Resist* 5**,** 1-8.
1333 Suvorova, E.S., Francia, M., Striepen, B., and White, M.W. (2015). A novel bipartite centrosome
1334 coordinates the apicomplexan cell cycle. *PLoS Biol* 13**,** e1002093.
1335 Tokuhiro, K., Hirose, M., Miyagawa, Y., Tsujimura, A., Irie, S., Isotani, A., Okabe, M., Toyama,
1336 Y., Ito, C., Toshimori, K., Takeda, K., Oshio, S., Tainaka, H., Tsuchida, J., Okuyama, A.,
1337 Nishimune, Y., and Tanaka, H. (2008). Meichroacidin containing the MORN motif is
1338 essential for spermatozoa morphogenesis. *J Biol Chem*.
1339 Trojan, P., Krauss, N., Choe, H.W., Giessl, A., Pulvermuller, A., and Wolfrum, U. (2008).
1340 Centrins in retinal photoreceptor cells: regulators in the connecting cilium. *Prog Retin*
1341 *Eye Res* 27**,** 237-259.
1342 Uilenberg, G. (2006). Babesia--a historical overview. *Vet Parasitol* 138**,** 3-10.
1343 Vaishnava, S., Morrison, D.P., Gaji, R.Y., Murray, J.M., Entzeroth, R., Howe, D.K., and
1344 Striepen, B. (2005). Plastid segregation and cell division in the apicomplexan parasite
1345 Sarcocystis neurona. *J Cell Sci* 118**,** 3397-3407.
1346 Vaughan, A.M., and Kappe, S.H.I. (2017). Malaria Parasite Liver Infection and Exoerythrocytic
1347 Biology. *Cold Spring Harb Perspect Med* 7.
1348 Vega, C.A., Buening, G.M., Green, T.J., and Carson, C.A. (1985). In vitro cultivation of Babesia
1349 bigemina. *Am J Vet Res* 46**,** 416-420.
1350 Wall, R.J., Roques, M., Katris, N.J., Koreny, L., Stanway, R.R., Brady, D., Waller, R.F., and
1351 Tewari, R. (2016). SAS6-like protein in Plasmodium indicates that conoid-associated
1352 apical complex proteins persist in invasive stages within the mosquito vector. *Sci Rep* 6**,**
1353 28604.
1354 Warrenfeltz, S., Basenko, E.Y., Crouch, K., Harb, O.S., Kissinger, J.C., Roos, D.S.,
1355 Shanmugasundram, A., and Silva-Franco, F. (2018). EuPathDB: The Eukaryotic
1356 Pathogen Genomics Database Resource. *Methods Mol Biol* 1757**,** 69-113.
1357 Watts, E., Zhao, Y., Dhara, A., Eller, B., Patwardhan, A., and Sinai, A.P. (2015). Novel
1358 Approaches Reveal that Toxoplasma gondii Bradyzoites within Tissue Cysts Are
1359 Dynamic and Replicating Entities In Vivo. *MBio* 6**,** e01155-01115.
1360 White, M.W., and Suvorova, E.S. (2018). Apicomplexa Cell Cycles: Something Old, Borrowed,
1361 Lost, and New. *Trends Parasitol* 34**,** 759-771.
1362 Worliczek, H.L., Ruttkowski, B., Schwarz, L., Witter, K., Tschulenk, W., and Joachim, A.
1363 (2013). Isospora suis in an epithelial cell culture system - an in vitro model for sexual
1364 development in coccidia. *PLoS One* 8**,** e69797.
1365
1366

1367 **Legend to Figures**

1368

1369 **Figure 1. Select apicomplexan phylogeny and division modes.** 18S ribosomal RNA based
1370 phylogeny of species whose division modes have been studied. *Cryptosporidium* spp. were used
1371 as outgroup. Bars on the right indicate different naming and biological relationships, with
1372 asexual division modes in blue and red. "in vacuole" and "in cytoplasm" indicate whether
1373 asexual replication occurs in a parasitophorous vacuole, or whether the parasite escapes from the
1374 vacuole and resides in the cytoplasm of the host cell for its replication. Note that only the acute
1375 stage merozoites of *S. neurona* replicates by endopolygeny in the cytoplasm, whereas metrocytes
1376 preceding the bradyzoites as well as the bradyzoites divide by endodyogeny within a vacuole
1377 supporting a proteoglycan cyst wall. Furthermore, tissue cysts for *C. suis* have not been
1378 described and this lacking ability is likely a secondary loss. In addition, for several *Plasmodium*
1379 spp. (Simonetti, 1996), as well as *Babesia* and *Theileria* spp. (Jalovecka et al., 2018) it has been
1380 shown that sporozoite formation progresses without karyokinesis to produce large polyploid
1381 nuclei while budding is from the cortex. We note that *Plasmodium* sporozoites infect hepatocytes
1382 wherein they divide by schizogony and manipulate the hepatocytes to expand their size, whereas
1383 *Theileria* sporozoites infect white blood cells, replicate by schizogony (Shaw and Tilney, 1992)
1384 and trigger white blood expansion as well as division (i.e. transformation, which basically is
1385 leukemia (Luder et al., 2009; Chakraborty et al., 2017), which contrasts with *Babesia* sporozoites
1386 as they directly infect red blood cells. "epg with kk" means "endopolygeny with karyokinesis",
1387 in case of *E. callospermophili*;"k.a." means "kinete amplification", in case of select *Babesia* spp.

1388

1389 **Figure 2. Apicomplexan asexual cell division by schizogony. A.** Schematic representation of
1390 progressive cell division steps during 'classic' schizogony. The mother's cytoskeleton (present in
1391 1) is disassembled following successful host cell invasion resulting in a pleomorphic cell (2)
1392 before onset of mitosis and karyokinesis, which can be asynchronous (3). Daughter cells bud
1393 from the cortex (4/5), positioned by the centrosome anchored at the plasma membrane (4). **B.**
1394 Schematic representation of phases in the cell division during schizogony with limited
1395 karyokinesis as seen during Heamosporidian sprorogenesis. Karyokinesis is inconsistently
1396 following each S/M-phase leading to a nuclei population with varying levels of ploidity. Note
1397 that nuclear cycles within the same nucleoplasm are similar (1), whereas budding is synchronous

1398 for all nuclei and linked to a final round of S/M (2). Note that the number of offspring in both
1399 forms of schizogony can reach into the 1000s, which is not represented in the schematics.
1400 Chromosome condensation does not occur and the chromosomes are only drawn to convey the
1401 principle of spindle pole attachment. Mother cytoplasm represented in grey, daughter cytoplasms
1402 in pink.
1403
1404 **Figure 3. Binary fission by *Babesia* spp**. **A-D.** *Babesia bigemina* iRBC stages. **A.**
1405 Immunofluorescence using MAb α-tubulin 12G10 (green) and TgCentrin1(red) polyclonal
1406 antibody. Centrin staining is not observed in interphase (G1) while diffuse and weak during cell
1407 division (cyt.). **B.** Immunofluorescence using MAb α-tubulin 12G10 (green) and microtubule
1408 (+)-end binding protein TgEB1 polyclonal antibody (red) demonstrates that the cortical
1409 microtubules are relatively short and do not reach the nucleus. **C.** Immunofluorescence using
1410 polyclonal guinea pig BbIMC1a antiserum (see Fig S1 for validation) and MAb α-tubulin 12G10
1411 shows the IMC is present during G/M, outlines budding daughters (cyt.), and extends along the
1412 length of the mature G1 parasites. * marks a recently invaded parasites wherein the cytoskeleton
1413 is completing disassembly; we observed many trophozoites without detectable PbIMC1a. **D.**
1414 Transmission electron microscopy of progressive iRBC developmental stages (1→6). Panel 1 is
1415 a disassembling merozoite already escaped from the vacuole displaying typical pattern of 6
1416 numbered remnants of the disassembling mother IMC. Panel 2 represents early daughter
1417 formation ('Mickey Mouse') with the nucleus being separated into the daughter buds. Panels 3,
1418 4, and 5 represent different sections though developing daughters where showing parallel
1419 assembly (in contrast to polar assembly) consistent with the angle under which the daughter buds
1420 assemble. Panel 6 displays two just divided daughters under the typical angle. N, nucleus, SB
1421 spherical body. Yellow marks IMC; orange arrows mark the typical angle and direction of
1422 daughter buds. Scale bars represent 500 nm. **E.** *Babesia divergens* basal complex upon
1423 completion of cell division. Scale bar represents 500 nm **F.** Schematic of apicomplexan asexual
1424 cell division by binary fission, which mechanistically represents a binary form of schizogony.
1425 Note that the mother's cytoskeleton is largely disassembled following successful host cell
1426 invasion resulting in a pleomorphic cell (2), but that fragments of the IMC are remaining
1427 throughout the division stages (2-4).

1428 **Figure 4. Apicomplexan asexual cell division by endodyogeny. A-E** show progressive steps of
1429 cell division as observed for *T. gondii* tachyzoites. Two daughters bud internally, while the
1430 mother's cytoskeleton is maintained and only destabilized just before emergence of nearly
1431 mature daughters (E). A dark blue SFA fiber anchors the centrosomes in the apex of the daughter
1432 buds.
1433
1434 **Figure 5. Endopolygeny with karyokinesis during merogony of *Cystoisospora suis*. A-D.**
1435 Parasites at different stages of endopolygeny. Acetylated (Ac) α-tubulin (red) marks the mother
1436 cells conoid (arrow heads in A, B), subpellicular microtubules, the spindle poles associated with
1437 nuclei undergoing mitosis, and the daughter conoids and subpellicular microtubules (C, D).
1438 Antiserum generated against TgNuf2 (green) marks the clustered kinetochores at mitotic
1439 spindles. A. Eight parasites at different stages in the division cycle. Green numbers indicate the
1440 number of spindle poles seen per mother cell, which is expanding non-geometrically in five of
1441 the parasites indicating asynchronous nuclear cycles. **B.** Five parasites at different stages of
1442 endopolygeny are shown. The parasite on the bottom has five nuclei: nuclei marked "M" are in
1443 early stages of mitosis as 2 spindle poles flanking a single 2N kinetochore cluster are seen; the
1444 circled nuclei represent just completed mitosis as the kinetochore clusters are relatively weak
1445 intensity (1N vs. 2N) and associated with only a single spindle pole. **C, D.** Two examples of cells
1446 at the synchronous daughter budding stage, which both produce 12 daughters as enumbered by
1447 the number of kinetochore clusters, again, consistent with non-geometric expansion of the nuclei.
1448 **E.** Schematic of apicomplexan asexual cell division by endopolygeny with karyokinesis. Note
1449 that the mitotic cycles of the nuclei in the same cytoplasm are not synchronous (2) resulting in
1450 non-geometrically expanded daughter numbers (4-5). Also note that the mother's cytoskeleton is
1451 maintained throughout the meront (technically 'schizont') stages and is only destabilized just
1452 before emergence of nearly mature daughters (5).
1453
1454 **Figure 6. Endopolygeny without nuclear fission by *Sarcocystis neurona* in the intermediate**
1455 **host. A.** Staining of progressive cell division cycle stages (1-4) with α-tubulin (green) marking
1456 the subpellicular microtubules of the mother cytoskeleton (arrow heads), the mitotic spindles (2b,
1457 right parasite; 3) and daughter merozoites subpellicular microtubules (4). Centrin staining (red)
1458 marks the centrosomes, which due to z-stack selection are not visible for all spindles/parasites.

1459 Scale bar applies across panels. **B.** Overexpression of a *Toxoplasma* YFP-IMC15 fusion protein
1460 (green) highlights the mother cell's cortical IMC sutures in both panels, whereas in further
1461 progressed panel 2 the bright internal spots mark the centrosomes poised for budding.
1462 Arrowhead marks the apical end of the mother parasite. Panel B modified from (Dubey et al.,
1463 2017). Scale bar applies across panels. **C.** Schematic of apicomplexan asexual cell division by
1464 endopolygeny without karyokinesis. Note the polyploid nuclei undergoing synchronized cycles
1465 of M-phase and mitosis resulting in geometrically expanded daughter cell numbers. Also note
1466 that the mother's cytoskeleton is maintained throughout the schizont stages (2-4) and is only
1467 destabilized just before emergence of nearly mature daughters (5).
1468

1469 **Figure 1**

1470

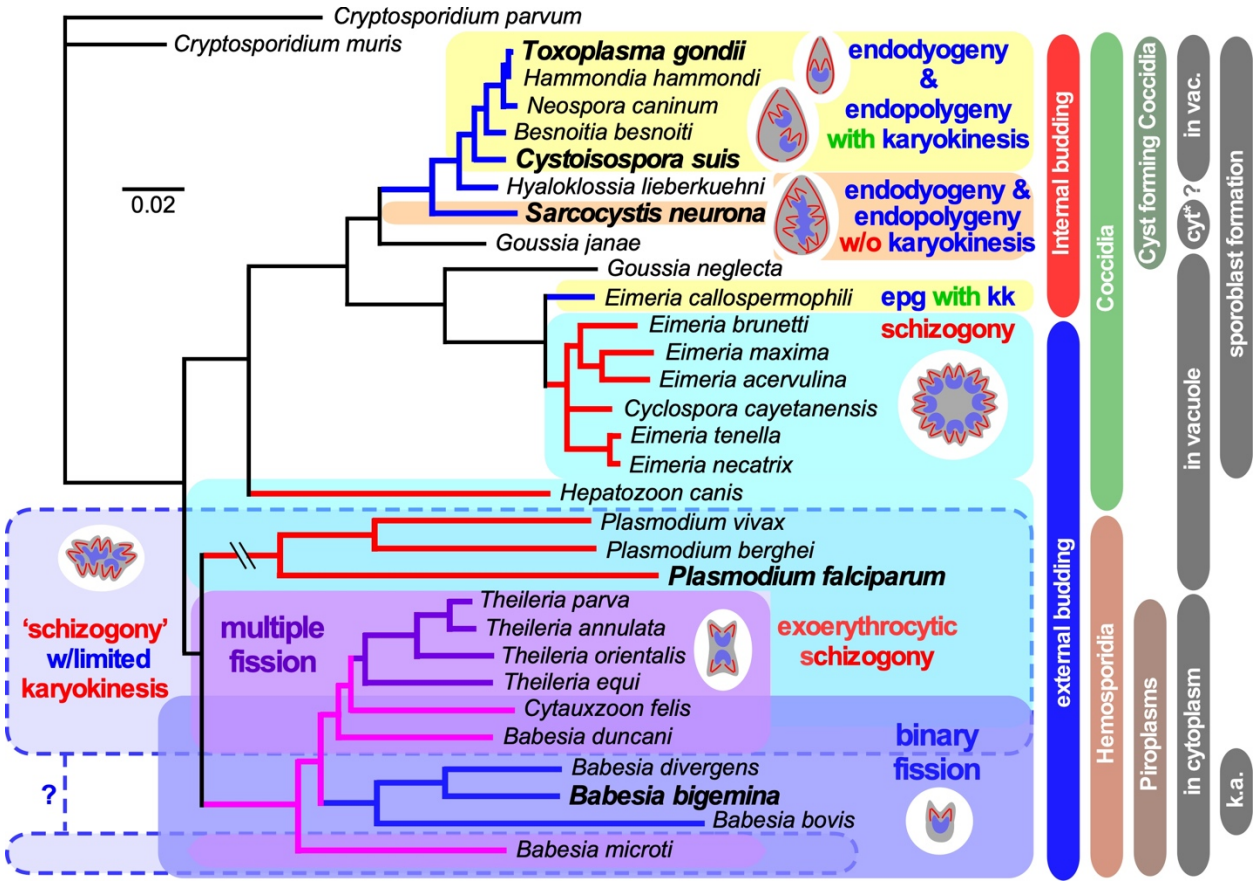

1471

1472 **Figure 2**

1473

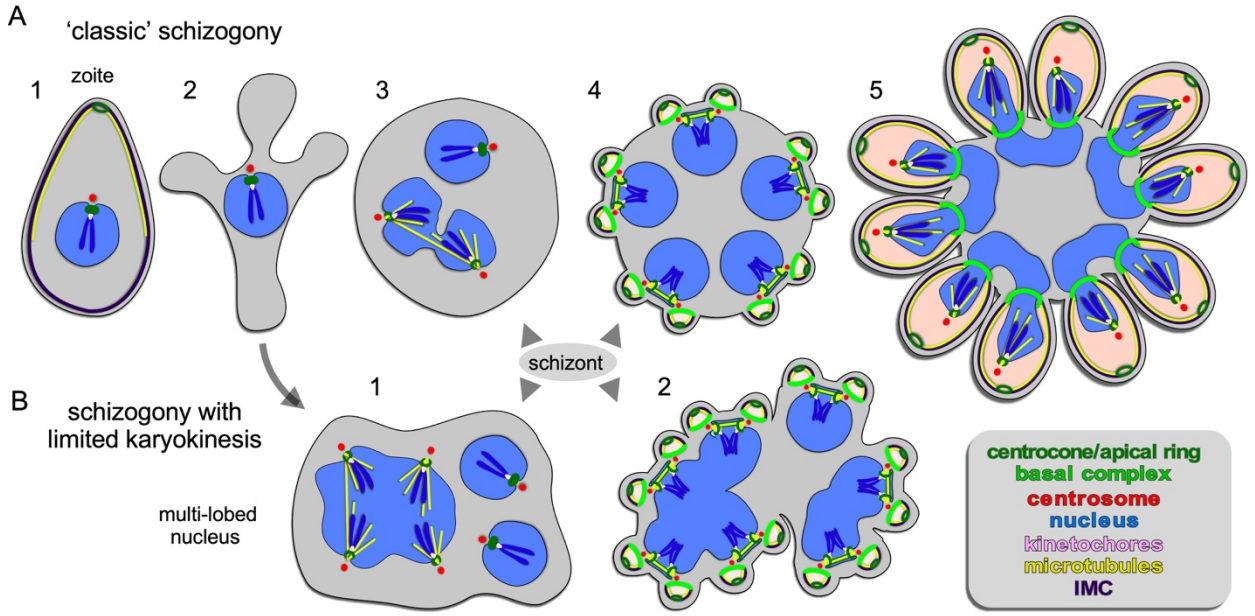

1474

1475 **Figure 3**

1476

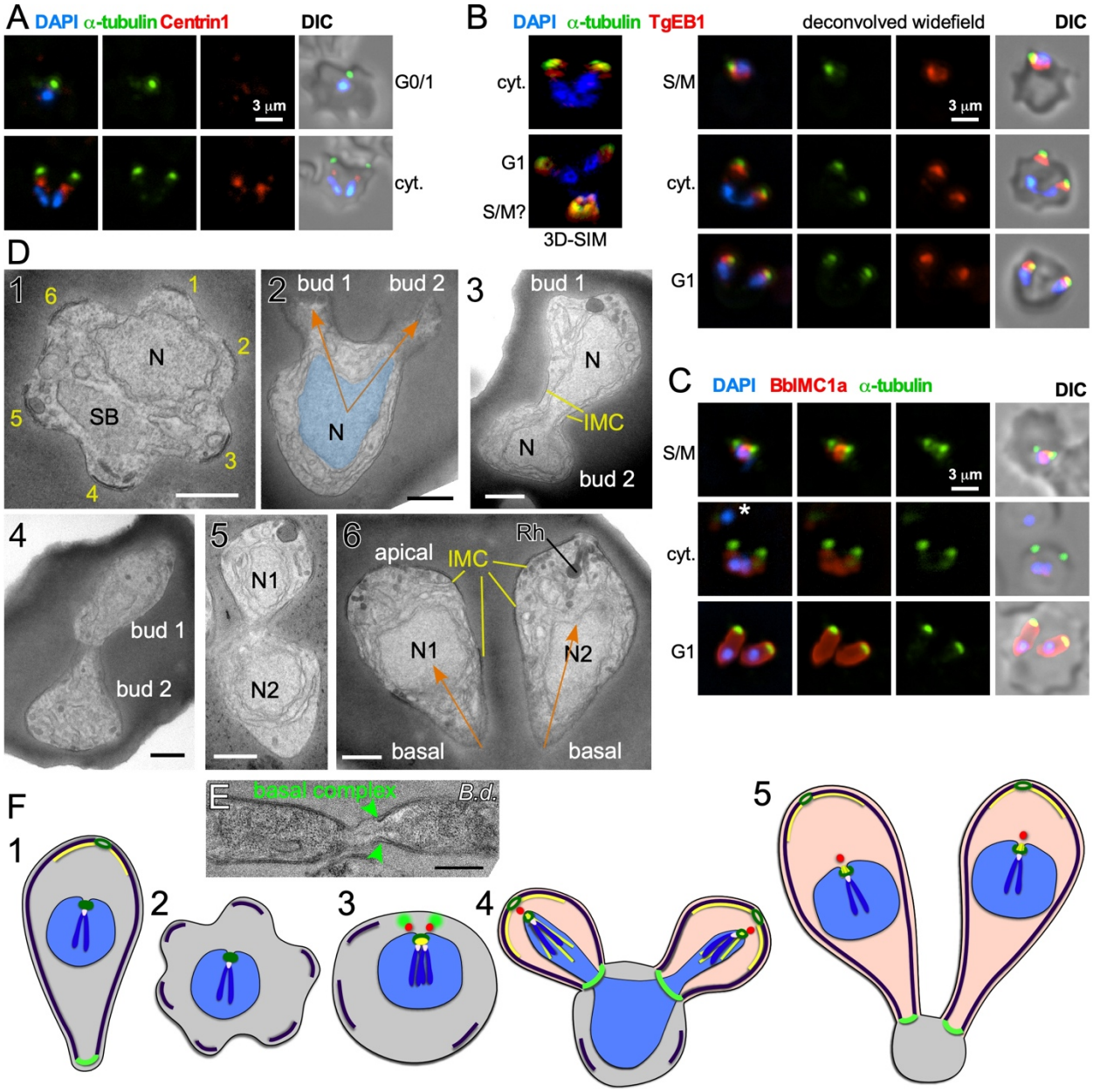

1477

1478 **Figure 4**

1479

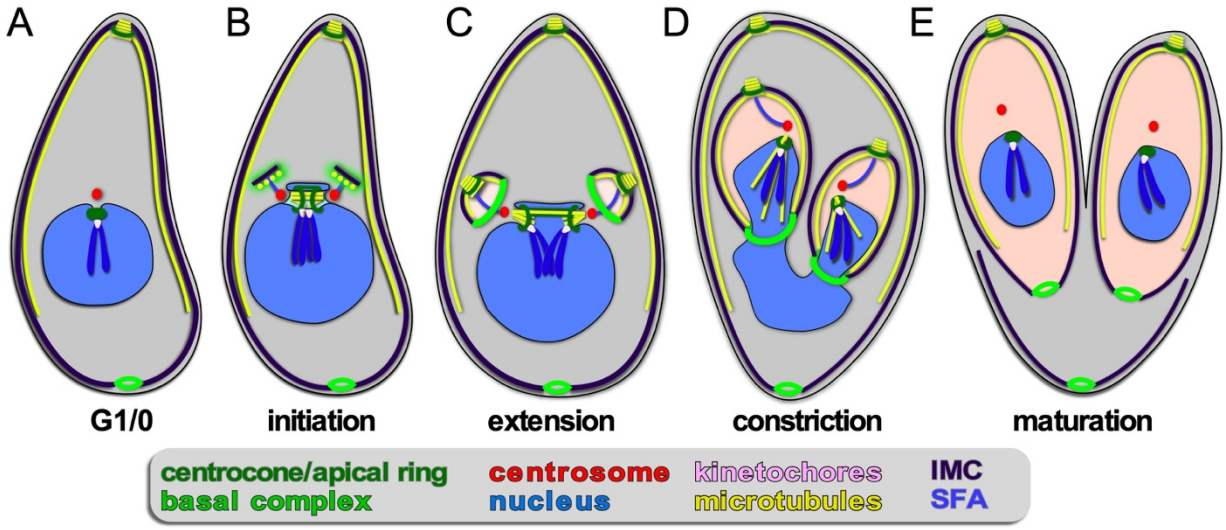

1480

1481 **Figure 5**

1482

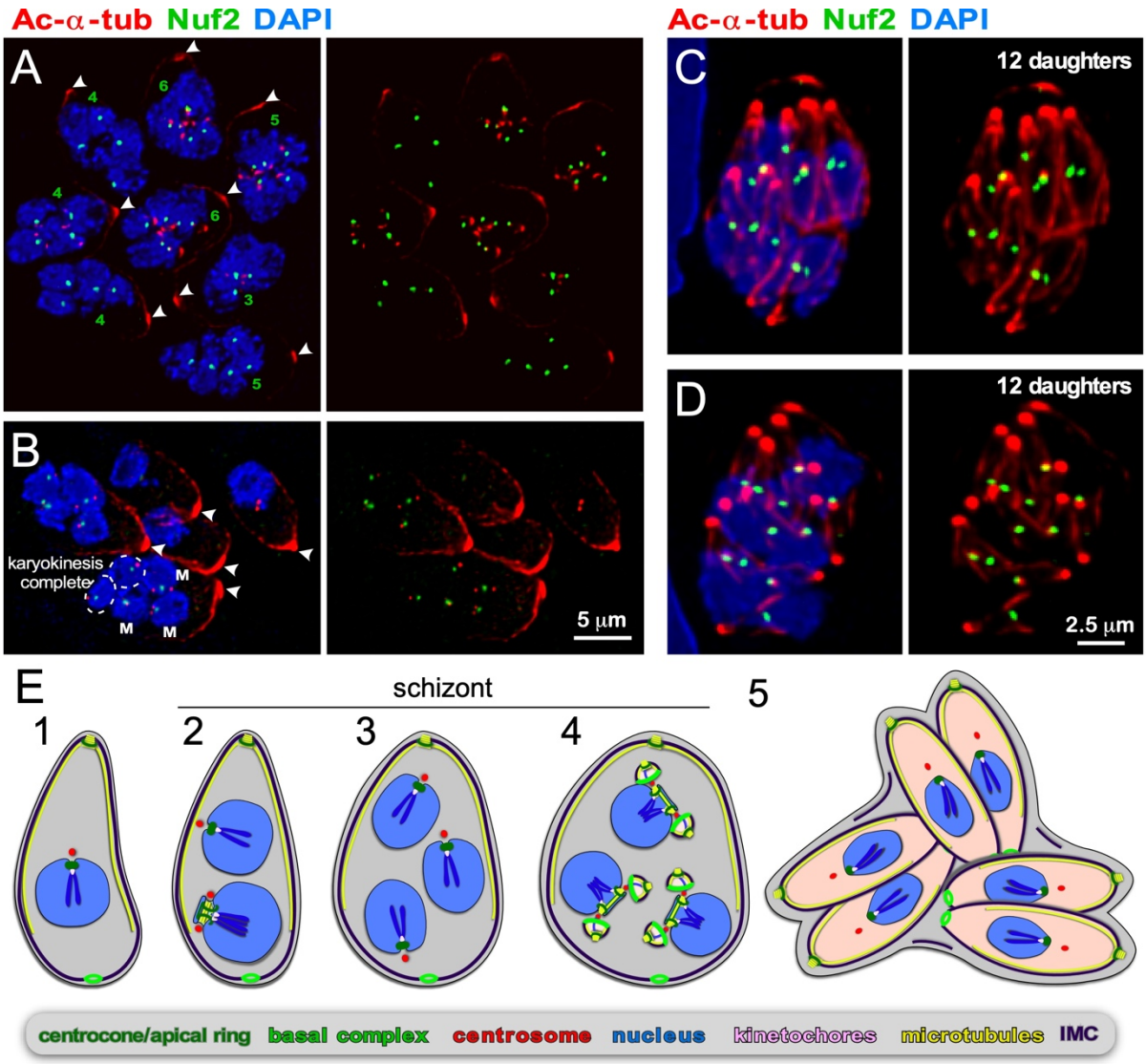

1483

1484 **Figure 6**

1485

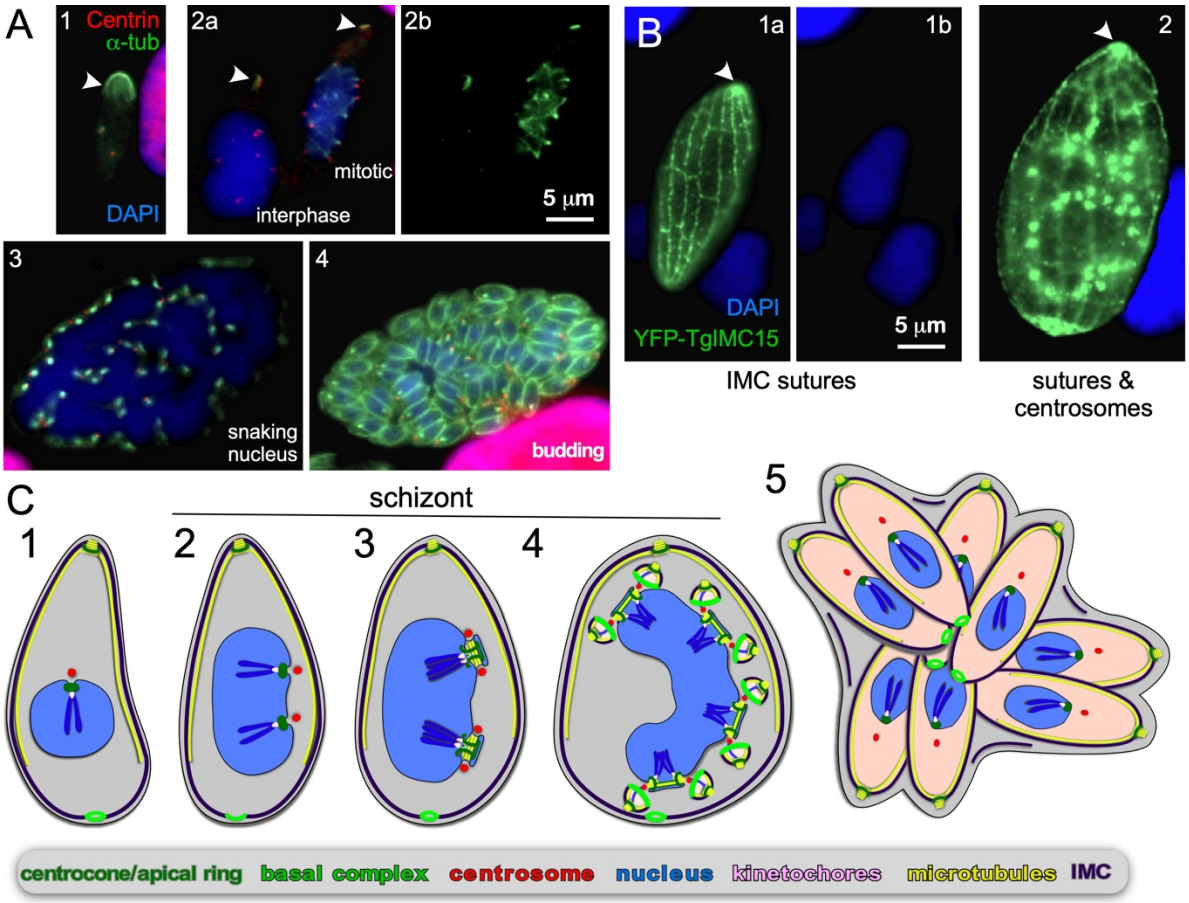

1486

1487 **Supplementary Material**

1488

1489 **Figure S1**

1490

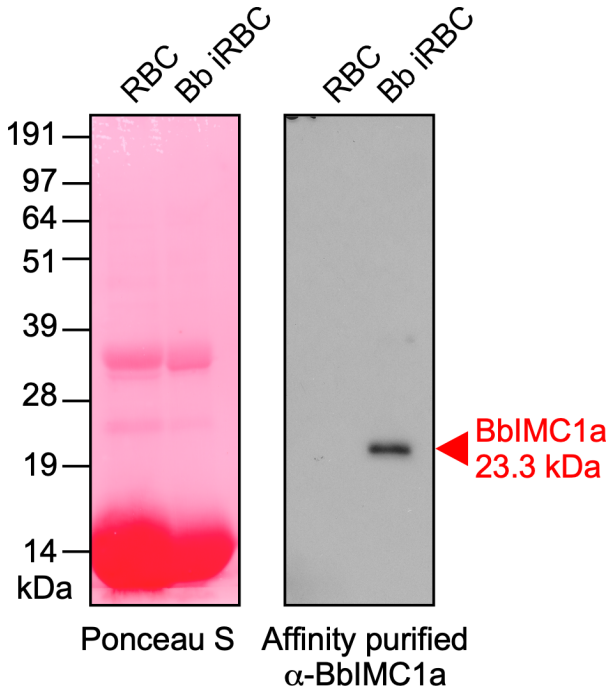

1491

1492

1493 **Figure S1. Validation of affinity purified guinea pig antiserum raised against recombinant**
1494 **His6-BbIMC1a by western blot.** Left panel: PonceauS staining of the western blot serving as
1495 loading control; Right panel: serum affinity purified against recombinant His6-BbIMC1a diluted
1496 1:250. RBC indicates cow red blood cell total lysate; Bb iRBC indicates total lysate of cow red
1497 blood cells with a *B. bigemina* parasitemia of 12%. Equal amounts of lysate were loaded across
1498 lanes. The predicted MW of BbIMC1a is 23.3 kDa.